

ZNF300 MAY INFLUENCE THE METASTATIC PROPERTIES IN
PANCREATIC DUCTAL ADENOCARCINOMA

by

Amanda Fisher

A thesis submitted to the Faculty of the University of Delaware in partial
fulfillment of the requirements for the degree of Master of Science in Biological
Sciences

Fall 2014

© 2014 Amanda Fisher
All Rights Reserved

UMI Number: 1585146

All rights reserved

INFORMATION TO ALL USERS

The quality of this reproduction is dependent upon the quality of the copy submitted.

In the unlikely event that the author did not send a complete manuscript and there are missing pages, these will be noted. Also, if material had to be removed, a note will indicate the deletion.



UMI 1585146

Published by ProQuest LLC (2015). Copyright in the Dissertation held by the Author.

Microform Edition © ProQuest LLC.

All rights reserved. This work is protected against unauthorized copying under Title 17, United States Code



ProQuest LLC.
789 East Eisenhower Parkway
P.O. Box 1346
Ann Arbor, MI 48106 - 1346

ZNF300 MAY INFLUENCE THE METASTATIC PROPERTIES IN
PANCREATIC DUCTAL ADENOCARCINOMA

by

Amanda Fisher

Approve:

Huey Jen Lee-Lin, Ph.D.
Professor in charge of thesis on behalf of the Advisory Committee

Approved:

Robin Morgan, Ph.D.
Chair of the Department of Biological Sciences

Approved:

George H. Watson, Ph.D.
Dean of the College of Arts and Sciences

Approved:

James G. Richards, Ph.D.
Vice Provost for Graduate and Professional Education

ACKNOWLEDGEMENTS

I would like to thank my advisor, Huey Lin, for this project. I truly feel that I have grown as a young scientist, professional, and individual.

Throughout the duration of my degree, the support that I have received by the Biology Department has been outstanding. Notably, Melinda Duncan, the Graduate Program Director, has provided a support system over the course of my journey. Equally supportive was Erica Selva, a professor who provided experimental and professional guidance more times than I can count. Having a professor like Dr. Selva, whom also served on my graduate committee, was something I consider myself fortunate to have had. Kenneth Van Golen, an additional committee member of which has researched pancreatic cancer, provided me with expertise and experimental suggestions to which I am grateful. Last, I would like to thank all the Biology Department staff, particularly Betty Cowgill, for ensuring my completion of the Biology Graduate Program requirements and for going beyond her duties to provide assistance to graduate students in our department.

Additionally, I would like to thank my colleagues, family, and friends. This journey has been life changing, and because of their support, I am able to move forward having successfully completed this program, with my sanity intact.

Last, I would like to thank previous lab members, Benjamin Rodriguez and Zhengang Peng, for their preliminary work of which my project stemmed from.

TABLE OF CONTENTS

LIST OF TABLES	vi
LIST OF FIGURES	vii
LIST OF ABBREVIATIONS	ix
ABSTRACT	x

Chapter

1	INTRODUCTION.....	1
	1.1 Pancreatic Cancer	1
	1.2 Pathology of PDAC	2
	1.3 Genetics of PDAC	4
	1.4 Epigenetics of PDAC	11
	1.5 Metastatic Process in PDAC	14
2	PRELIMINARY WORK.....	19
	2.1 Genome Wide Methylation Profile	19
	2.2 ZNF300 as a Candidate Hypermethylated Gene	21
	2.3 Hypothesis	28
3	METHODS AND MATERIALS	29
	3.1 Cell Culture	29
	3.2 Protein Isolation	30
	3.3 Western Blotting	30
	3.4 RNA Isolation	32
	3.5 cDNA Synthesis.....	33
	3.6 Quantitative Reverse Transcription Polymerase Chain Reaction	34
	3.7 DNA Isolation.....	35
	3.8 Bisulfite Conversion	36
	3.9 Bisulfite Converted Polymerase Chain Reaction.....	36
	3.10 Combined Bisulfite Restriction Enzyme Analysis (COBRA).....	37
	3.11 Transformations of Bisulfite PCR.....	39
	3.12 Mini Preps.....	40
	3.13 Retroviral Infections	41
	3.14 Transwell Migration Assay.....	43

4	RESULTS	44
4.1	Validation of Methylation within the CpG Island of ZNF300	44
4.2	Correlation of ZNF300 Methylation and Expression	46
4.3	Role of ZNF300 in PDAC Metastasis	54
5	DISCUSSIONS AND FUTURE DIRECTIONS	62
	REFERENCES	68
	Appendix	80
	A. LETTERS OF PERMISSIOIN	80
	B. COPYRIGHTED WORKS	82

LIST OF TABLES

Table 1.1 Common mutations in PDAC.....	10
Table 3.1 Antibodies utilized to detect protein expression	32
Table 3.2 Primer sequences used in qRT-PCR	35
Table 3.3 COBRA primers for ZNF300 CGI	37
Table 3.4 Sequencing primers for Topo®TA vector	41

LIST OF FIGURES

Figure 1.1	Histological progression of PanIN precursor lesions to PDAC	3
Figure 1.2	The genetic progression model for (PDAC)	9
Figure 1.3	Stages of metastasis	17
Figure 1.4	Role of tumor microenvironment in PDAC	18
Figure 2.1	Schematic of FG and L3.6pl cell line generation used in GWMP	23
Figure 2.2	CGI methylation in non-malignant and PDAC cell lines as indicated by COBRA	24
Figure 2.3	Overall methylation of the ZNF300 CGI in PDAC lines.....	25
Figure 2.4	Luciferase reporter assay under the ZNF300 promoter	26
Figure 2.5	Immunohistochemical staining of ZNF300 in paraffin-embedded patient tissues	27
Figure 3.1	The ZNF300 CGI forward sequence	39
Figure 4.1	DNA methylation within the ZNF300CGI in FG, L3.6pl, as measured by COBRA.....	47
Figure 4.2	Influence of cell passage towards DNA methylation with the CGI of ZNF300 using COBRA.....	48
Figure 4.3	Bisulfite sequencing of ZNF300CGI in FG and L3.6pl over cell passage	49
Figure 4.4	Averaged ZNF300 CGI methylation in FG and L3.6pl cells.....	50
Figure 4.5	ZNF300 transcript levels in FG and L3.6pl quantified via qRT-PCR	51

Figure 4.6	ZNF300 expression in FG and L3.6pl cell lines over time in culture.....	52
Figure 4.7	Methylation versus ZNF300 expression correlation plot.....	53
Figure 4.8	Cell migratory abilities of FG and L3.6pl cells via transwell migration assays.....	57
Figure 4.9	Schematic of ZNF300 overexpression in L3.6pl-Tet cells via the Tet-On retroviral expression system	58
Figure 4.10	Luciferase activity following DOX-induced luciferase expression	59
Figure 4.11	ZNF300 transcript levels following DOX induction using the Tet-On retroviral expression system	59
Figure 4.12	ZNF300 expression over time following DOX induction using the Tet-On retroviral expression system.....	60
Figure 4.13	Cell migration following DOX-induction of ZNF300 expression using the Tet-On retroviral expression system.....	61

LIST OF ABBREVIATIONS

PDAC	pancreatic ductal adenocarcinomas
PanINs	pancreatic intraepithelial neoplasms
KRAS2	Kirsten Rat Sarcoma Viral Oncogene Homolog
CDK	cyclin-dependent kinase
TGF β	transforming growth factor β
CpG	cytosine-guanine
EMT	epithelial-to-mesenchymal transition
ECM	extensive extracellular matrix
GWMP	genome-wide DNA methylation
MiGS	MBD-isolated Genome Sequencing
COBRA	Combined Bisulfite Restriction Analysis
ZNF300	Zinc Finger Protein 300
CGI	validate CpG island
FG	fast-growing
qRT-PCR	Quantitative reverse transcription polymerase chain reaction
PCR	polymerase chain reaction
L3.6pl-Tet	L3.6pl cells stably expressing the pRetro-Tet-ON vector
+ZNF300	L3.6pl-Tet cells with Tre3G-ZNF300
EV	empty vector Tre3G
+LUC	Tre3G containing Luciferase
Tre3G-ZNF300	ZNF300 driven under a Tre3G promoter
DOX	doxycycline
UT	untransfected cell

ABSTRACT

Aberrant DNA methylation of promoter CpG islands (CGI) is a contributing factor that facilitates the dysregulation of gene expression to promote the tumorigenesis of pancreatic ductal adenocarcinoma (PDAC). Moreover, due to the overwhelming number of PDAC patients presented with metastasis at the time of diagnosis, it is necessary to better understand the process of metastasis. To understand the role of DNA methylation may in the metastasis of PDAC, two isogenic cells lines, generated by Dr. Isaiah Fidler at the University of Texas MD Anderson Cancer Center, were used as a cell culture model. These cell lines were generated from orthotopic injections of an established pancreatic cancer cell line, colo357, into the pancreas of nude mice. Upon injection, metastasis formed in the liver. Metastatic cells from the metastases were isolated and grown in culture to yield a lowly metastatic cell line, fast growing (FG). This process was repeated using FG cells, and after three rounds of injection and isolation, the enriched metastatic cells were isolated to yield a highly metastatic variant, L3. 6. Preliminary work, performed by previous lab members, identified genes exhibiting promoter hypermethylation in a high metastatic cell line, L3.6pl, compared to the lowly metastatic isogenic variant cell line, FG. One of those genes, ZNF300, was chosen as a candidate gene for many reasons. First, analysis of percent methylation within the ZNF300 CGI indicated increased methylation among L3.6pl cells compared to FG, specifically sixteen percent to one

percent, respectively. In addition to increased methylation, the region of the ZNF300 promoter that was hypermethylated was also shown to affect promoter activity according to luciferase promoter assays. Therefore, it was hypothesized that the observed hypermethylation in L3.6pl cells may lead to decreased ZNF300 expression. Moreover, ZNF300 expression was identified in pancreatic tumor samples from ten PDAC patients via immunohistochemical staining; however, analysis from lymph node metastases from many of these patients showed diminished ZNF300 expression compared to the primary tumor. Taken together, this data supports our overall goal to determine if ZNF300 hypermethylation correlates to ZNF300 expression, and more importantly, if this correlation is related to the metastatic ability of L3.6pl cells.

To determine if ZNF300 is epigenetically regulated, methylation levels were quantified via COBRA and bisulfite sequencing in both FG and L3.6pl cells. Additionally, ZNF300 expression was measured via qRT-PCR and western blotting analysis. To determine the functional role of ZNF300 in the metastatic process of L3.6pl, we attempted to overexpress ZNF300 using the p-RetroX-Tre3G Tet-ON inducible expression system. Following induction using doxycycline, both the expression and migratory ability were measured.

The data in this study concludes that, contrary to preliminary data, the ZNF300 CpG island is not differentially methylated in L3.6pl cells compared to FG cells. Our expression data is in accordance with the methylation levels, and thus, indicated no significant difference in ZNF300 expression between the two isogenic variant cell lines. Moreover, we were unable to induce ZNF300 expression using the retroviral

inducible system, but rather noted potentially off target effects of doxycycline in infected L3.6pl cells. Due to our inability to induce ZNF300 expression, we are unable to identify the role of ZNF300 in the metastatic process of PDAC.

Chapter 1

INTRODUCTION

1.1 Pancreatic Cancer

Pancreatic cancer is among the top causes of adult related cancer deaths according to the most recent statistics released by the National Cancer Institute in 2014 (Siegel, Ma, Zou, & Jemal, 2014). While the number of disease-related fatalities is currently ranked fourth among all cancer types, pancreatic cancer exhibits the lowest five-year survival rate; for every 100 people diagnosed only six live past five years of life (Siegel, Ma, Zou, & Jemal, 2014). Physiologically, the pancreas is a gland consisting of two generalized functions. First, the endocrine function is carried out via the islet of Langerhans which release both insulin and glucagon to regulate blood glucose levels (Hezel, Kimmelman, Stanger, Bardeesy, & Depinho, 2006). Secondly, the exocrine function is executed by acinar cells which secrete enzymes into pancreatic ducts that aid in digestion upon reaching the duodenum (Hezel, Kimmelman, Stanger, Bardeesy, & Depinho, 2006). While there are various types of pancreatic carcinomas, 90 percent of incidents result from abnormal proliferation of epithelial cells lining pancreatic ducts (Hruban, Maitra, & Goggins, 2008). Due to their location and gland-like morphology, malignancies originating from pancreatic ducts are termed pancreatic ductal adenocarcinomas (PDAC) (Hruban, Maitra, & Goggins, 2008). It is known that PDAC

originates from non-invasive precursor lesions including pancreatic intraepithelial neoplasms (PanINs), intraductal papillary mucinous neoplasms, intraductal tubulopapillary neoplasms, and mucinous cystic neoplasms (Maitra, Fukushima, Takaori, & Hruban, 2005). These precursors differ in pathology as well as location; specifically, most precursors originate from different ducts within the pancreas (Longnecker et al., 2005). The most prevalent subtype that gives rise to PDAC is PanINs, neoplasms that originate from microscopic ducts within the pancreas (Hruban et al., 2001). Of patients with adenocarcinomas, approximately eighty-two percent have PanIN lesions. For this reason, and because the etiology of this precursor is the most understood, this will be the primary focus in sections to follow.

1.2 Pathology of PDAC

The pathological progression from preinvasive PanIN lesions to PDAC has been categorized into three stages, shown in Figure 1.1 (Hruban et al., 2001). In the first stage, PanIN1A, cuboidal epithelium lining microscopic ducts transition into columnar-like epithelia. PanIN1B lesions are similar to PanIN1A, however are further distinguished by the formation of micro-papillary extensions and may have epithelia that are pseudostratified in nature (Hruban et al., 2001; Hruban et al., 2004). With increasing dysplasia, characteristics of PanIN2 lesions develop including: prominent papillary extensions, a partial loss of cell polarity, and nuclear anomalies (Hruban et al., 2001; Hruban et al., 2004). The last and most severe precursor that gives rise to PDAC, PanIN3, displays extreme nuclear atypia, and mostly papillary architecture that is

often accompanied with epithelial “budding” or cribriform extensions into the lumen (Hruban et al., 2001). This stage is said to resemble carcinoma histologically but is unable to invade beyond the epithelial membrane (Hruban et al., 2001; Hruban et al., 2004).

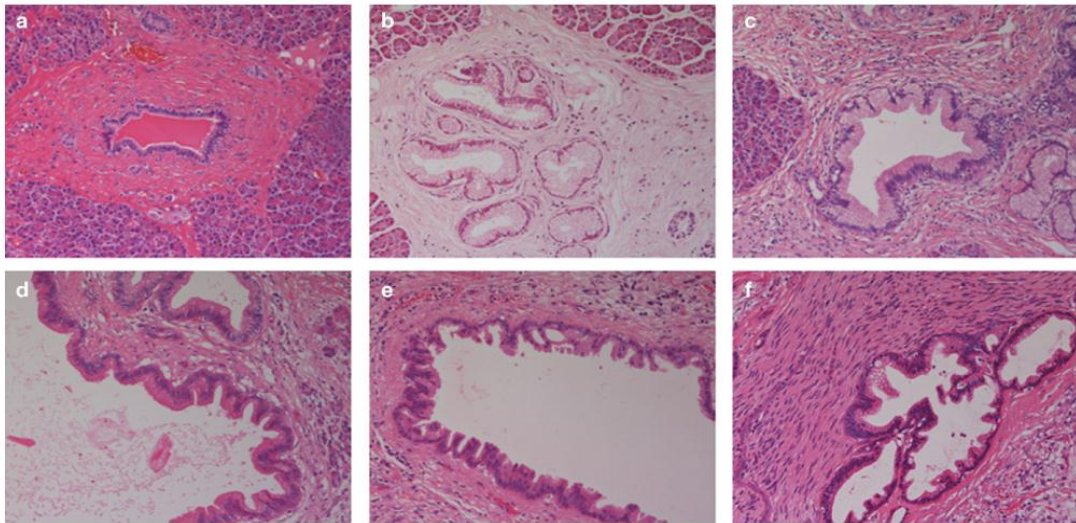


Figure 1.1 Histological progression of PanIN precursor lesions to PDAC. Normal pancreatic ducts (A) are lined with epithelial cells that transition from cuboidal to columnar (B) in PanIN-1A. PanIN-1B is accompanied by micropapillary formation(C) of which become more prominent in PanIN-2(D). With increasing neoplasia, cellular complexity accentuates and eventually leads to the last stage prior to carcinoma, PanIN-3 (E). The hallmark of invasive carcinoma is the appearance of cribriform development (F). Figure adapted from Saiki and Horii, (2014).

1.3 Genetics of PDAC

The advancement of normal human cells into a neoplastic state results from dynamic genetic alterations including point mutations, chromosomal rearrangements, and copy number variants (FOULDS, 1954; Hanahan & Weinberg, 2000; Nowell, 1976). Successive accumulation of these genetic insults facilitates the acquisition of the tumorigenic properties normal cells need to reach the irreversible state of carcinogenesis (FOULDS, 1954; Hanahan & Weinberg, 2000; Nowell, 1976). Many efforts have been made to identify somatic events that are “drivers” of tumorigenesis from those that are secondary effects or “passengers” (Carter, Samayoa, Hruban, & Karchin, 2010; Greenman et al., 2007; S. Jones et al., 2008). One such study, performed by Jones et al., 2008, showed that PDAC patients harbor a greater percentage of point mutations than both copy number variants and deletions (S. Jones et al., 2008). Of these, the Kirsten Rat Sarcoma Viral Oncogene Homolog (*KRAS2*) gene has been identified as the most commonly mutated driver gene in PDAC; apparent in approximately ninety percent of patients with PanIN lesions and ninety-five percent of patients with PDAC (Caldas & Kern, 1995; Kanda et al., 2012).

Functionally, *KRAS2* encodes for the GTPase, KRAS, which serves as an effector protein for a host of signaling pathways (S. L. Campbell, Khosravi-Far, Rossman, Clark, & Der, 1998). Upon phosphorylation of an upstream receptor, KRAS undergoes a conformational change from an unbound-GDP, inactive state to a bound-GTP, active

state (Bourne, Sanders, & McCormick, 1990; Bourne, Sanders, & McCormick, 1991). When active, KRAS targets downstream effector proteins that ultimately lead to changes in cell cycle progression, proliferation, and cell differentiation (S. L. Campbell, Khosravi-Far, Rossman, Clark, & Der, 1998). The signal is then extinguished by unphosphorylation of GTP to GDP. Most often, PDAC patients harbor *KRAS2* point mutations within codon 12, an event that inevitably compromises the GTPase ability of KRAS and renders it constitutively GTP-bound and active (Bourne, Sanders, & McCormick, 1990; Miglio et al., 2014; C. Shi et al., 2008). Oncogenic KRAS activity leads to an increase a number of signaling cascades that drive tumorigenesis such as mitogen-activated protein kinases extracellular-signaling receptor kinase, p38 MAP Kinase, and the phosphoinositol-3 kinase pathway (Edling et al., 2010; Eser, Schnieke, Schneider, & Saur, 2014; Pylayeva-Gupta, Grabocka, & Bar-Sagi, 2011; Yamamoto et al., 2004).

The dominant nature of this driver gene in PDAC promotion is supported by studies using mouse models harboring *KRAS2* mutations (Aguirre et al., 2003; Collins, Brisset et al., 2012; Herreros-Villanueva, Hijona, Cosme, & Bujanda, 2012; Hingorani et al., 2003). Consistent with these findings, it has been recently reported that mice expressing oncogenic *KRAS^{G12D}* in pancreatic progenitor cells manifest penetrant PanIN lesions (Collins, Brisset et al., 2012; Collins, Bednar et al., 2012). Interestingly, when oncogenic KRAS was turned off, these PanIN lesions regressed (Collins, Bednar et al., 2012). This data suggests that oncogenic KRAS is needed to not only initiate PanIN lesion development, but maintain precursor stages (Collins, Bednar et al., 2012). While oncogenic KRAS plays a critical role in tumorigenesis, dysfunctional KRAS

expression alone is not sufficient for carcinogenesis, suggesting that additional genetic insults are necessary to reach PDAC (Aguirre et al., 2003; Collins, Bednar et al., 2012).

Fearon and Vogelstein proposed roughly 4-5 genetic events are necessary to transform normal epithelium into invasive carcinoma (Fearon & Vogelstein, 1990; FOULDS, 1954; Hanahan & Weinberg, 2000). The genetic events associated with PDAC include activation of oncogenic KRAS in early stages of progression, in concert with a deactivation of tumor suppressor genes in the intermediate to late stages (Hezel, Kimmelman, Stanger, Bardeesy, & Depinho, 2006; Hruban, Iacobuzio-Donahue, Wilentz, Goggins, & Kern, 2001; Maitra & Hruban, 2008). The most frequently dysregulated tumor suppressor protein in PDAC is P16, encoded by the *CDKN2A* gene (Caldas et al., 1994; Rocco & Sidransky, 2001; Rozenblum et al., 1997). Studies have shown nearly ninety-five percent of patients with PDAC harbor a loss of P16 expression, which occurs through a variety of molecular mechanisms (Maitra & Hruban, 2008; Rozenblum et al., 1997; Schutte et al., 1997a). In a normal cell, P16 regulates the formation of the cyclin-dependent kinase (CDK) 4,6-cyclin D complex (M. Serrano, Hannon, & Beach, 1993). Inhibition of CDK4,6-cyclin D blocks retinoblastoma (Rb) protein phosphorylation, and promotes formation of the repressive complex Rb-E2F, and transcriptional impediment of cycle cell progression genes (H. S. Zhang, Postigo, & Dean, 1999). Preventing transcriptional activation of target genes is necessary for cell cycle progression (Hanahan & Weinberg, 2000). Thus by decreasing P16 expression, cancer cells gain the ability to sustain proliferation, a requisite characteristic needed for carcinogenesis (Hanahan & Weinberg, 2000; Liggett & Sidransky, 1998; Rocco & Sidransky, 2001).

In the latter stages of PanIN progression there is aberrant expression of additional tumor suppressor proteins, including P53, encoded by the *TP53* gene. Functionally, P53 serves as a transcription factor that regulates numerous cellular processes including: cell cycle arrest, maintenance of DNA integrity, apoptosis, and autophagy (Zilfou & Lowe, 2009). Loss of P53 expression resulting from *TP53* deletions can occur; however, point mutations, specifically within the DNA binding region of *TP53*, are most common (Kanda et al., 2013; Morton et al., 2010; Olivier et al., 2002). These point mutations often affect the stability of P53, its DNA binding affinity, and tumor suppressive functions (Bullock, Henckel, & Fersht, 2000). Interestingly, some mutant forms of P53 exhibit a gain-of-function in many cancers and exhibits oncogenic activity (Kastan & Berkovich, 2007; Y. Li & Prives, 2007). It has been shown that PDAC patients expressing mutant forms of P53, both a gain and loss of P53, have a poor prognosis (Ansari, Rosendahl, Elebro, & Andersson, 2011; Kanda et al., 2013). This correlation is supported by recent data suggesting mutant P53 can promote invasion and metastasis of pancreatic carcinomas in murine models (Ansari, Rosendahl, Elebro, & Andersson, 2011; Weissmueller et al., 2014).

The last gene implicated in PDAC, *DPC4*, is often mutated in the later stages of PanIN progression (Hezel, Kimmelman, Stanger, Bardeesy, & Depinho, 2006; R. E. Wilentz et al., 2000). Loss of expression of the *DPC4* gene product, SMAD4, is correlated with even poorer patient outcome (Blackford et al., 2009). Recently, SMAD4 has been identified as a predictive marker of lymph node metastasis via proteomic analysis of PDAC patient tumors (Blackford et al., 2009; Oshima et al., 2013).

Approximately fifty-five percent of patients with PDAC carry *DPC4* mutations (Blackford et al., 2009). Of these, thirty percent exhibit homozygous deletions, while the remaining twenty-five percent carry point mutations accompanied by a loss of heterozygosity of the intact allele (Schutte et al., 1996; R. E. Wilentz et al., 2000). Functionally, SMAD4 acts as a transcriptional activator that induces expression of growth arrest genes via the transforming growth factor β (TGF β) pathway (Massague, Blain, & Lo, 2000). Upon ligand binding to TGF β receptors, downstream effector proteins become phosphorylated whereby they can oligomerize with SMAD4 and translocate to the nucleus (Y. Shi & Massagué, 2003). Many PDAC patients harbor point mutations that compromise the ability of SMAD4 to interact with binding partners, leading to an abrogation of cell cycle regulation (Massague, Blain, & Lo, 2000; Miyaki & Kuroki, 2003).

In summary, there are four genes known to drive the progression of pre-invasive PanIN lesions to PDAC, shown in Figure 1.2. While only *KRAS2* mutations have been shown to induce PanIN lesions independently, PDAC requires the inactivation of P16 in intermediate stages of PanIN development, in concert with genetic changes that leads to loss of P53 and SMAD4 dysregulation in the later stages of PanIN development (Hezel, Kimmelman, Stanger, Bardeesy, & Depinho, 2006). There are other mutations that are associated with pancreatic cancer; however, their independent role in PDAC development is not as well known. There have been studies that have sequenced whole-exomes from pancreatic tumor samples and have identified other significantly mutated genes in pancreatic cancer (A. V. Biankin et al., 2012; S.

Jones et al., 2008). The genes identified in these exome studies, and their function, are summarized in Table 1.1.

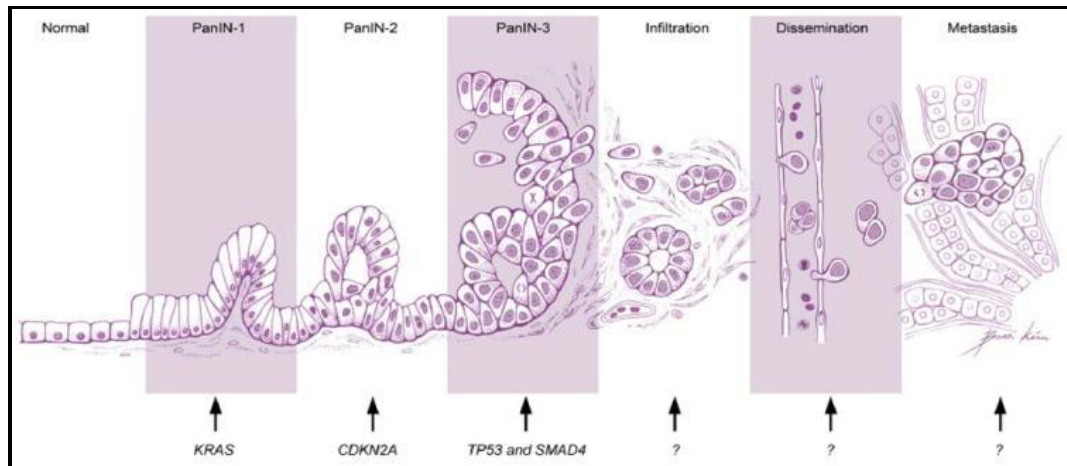


Figure 1.2 The genetic progression model for (PDAC). In stage 1, KRAS mutations drive the initiation and maintenance of PDAC. With increasing dysplasia, tumor suppressors are often silenced- the most common being a loss of p16 in stage 2. In stage 3, mutations in p53 and SMAD4 compromise tumor suppressor function and consequently promote the carcinogenic state. Other genes that may drive successive stages such as infiltration, dissemination, and metastasis are not as well understood. (Iacobuzio-Donahue, CA et al., 2012)

Table 1.1 Common mutations in PDAC. Exome sequencing performed by Biankin et al., 2012, identified significantly mutated genes in patients with pre-operable sporadic pancreatic ductal adenocarcinomas compared to normal matched tissues.

Mutated Gene	Generalized Function
KRAS	GTPase in MAPK pathway
TP53	Regulatory protein in DNA damage response,
CDKN2A	Regulates G1/S phase of cell cycle
SMAD4	TGF β pathway; Induces expression of genes that negatively regulate growth
MLL3	Transcriptional regulatory protein
TGF β R2	Receptor in TGF β pathway
ARID1A	Part of SNF/SWI complex; Chromatin remodeling
ARID2	Part of PBAF complex; Chromatin remodeling
EPC1	Part of NuA4 histone acetyltransferase complex;
ATM	DNA damage response
SF3B1	Part of U2 snRNP; mRNA splicing
ZIM2	Transcription factor; Imprinted gene
MAP2K4	MAPK protein kinase
NALCN	Non-selective cation channel
SLC16A4	Transporter for various monocarboxylates
MAGEA6	Ligase stability protein

*Figure adapted from data reported by Biankin et al., 2012.

1.4 Epigenetics of PDAC

There have been advancements made towards the identification of somatic mutations that drive tumorigenesis of PDAC; however, there are additional genomic alterations that promote PDAC development without modifying the DNA sequence (Esteller, 2008; Feinberg & Tycko, 2004). These regulatory mechanisms encompass the field of epigenetics, or the study of heritable changes in gene expression mediated by events that do not alter the genomic sequence (Esteller, 2008; Feinberg & Tycko, 2004). Two common types of epigenetic events involve the addition of chemical groups to impede DNA accessibility, and ultimately, can reduce the transcriptional activity of genes (Esteller, 2008). Specifically, chemical groups can be added to histone proteins, or DNA itself (Esteller, 2008). An example is the addition of acetyl groups (-COCH₃) to lysine (K) amino acids of histone tails (S. L. Berger, 2002; D. M. PHILLIPS, 1963). This modification neutralizes the attraction of negatively charged DNA to the positively charged histone complex (J. D. Anderson, Lowary, & Widom, 2001; D. M. PHILLIPS, 1963). Depending on the number of acetyl groups added, the compaction of DNA around histone complexes changes and subsequently, alters the accessibility of transcriptional machinery to gene coding regions (J. D. Anderson, Lowary, & Widom, 2001; S. L. Berger, 2002).

In addition to histone modifications, epigenetic marks can also be added to DNA (Esteller, 2008). Specifically, methyl groups (-CH₃) can be covalently attached to cytosine-guanine (CpG) dinucleotides at the fifth position of the cytosine ring

(HOTCHKISS, 1948; L. D. Moore, Le, & Fan, 2013). The enzymes that carry out covalent addition of methyl groups are DNA methyltransferase enzymes. Specifically, DNA methyltransferase I maintains methylation patterns of newly synthesized DNA during DNA replication, and DNA methyltransferase 3A and B carry out *de novo* methylation (Bestor, Laudano, Mattaliano, & Ingram, 1988; M. Okano, Bell, Haber, & Li, 1999).

CpG dinucleotides are not evenly distributed throughout the genome, but rather clustered in regions referred to as CpG islands (Gardiner-Garden & Frommer, 1987) . When CpG islands are located in gene regulatory sequences, such as promoters or enhancers, they are predominantly unmethylated across many cell types (Edwards, 1990; Gardiner-Garden & Frommer, 1987). Typically, CpG islands are associated with transcriptionally active genes, such as housekeeping genes, and exhibit low levels of methylation (Takai & Jones, 2002; M. Weber et al., 2007). Despite this fact, methylation has been shown to regulate critical processes including X-inactivation and early embryogenesis up until blastocyst stage (Bird, 2002; Hackett & Surani, 2013). Additionally, aberrant methylation patterns have been linked to disease etiology, including cancer (Feinberg & Vogelstein, 1983; Feinberg & Tycko, 2004).

Hypermethylated CpG islands located in gene promoter regions are prevalent in numerous cancer subtypes, including PDAC (P. A. Jones & Baylin, 2002; Vincent et al., 2011). Promoter hypermethylation facilitates tumorigenesis by impeding transcription factor binding and decreasing the transcription of tumor suppressor genes (Razin & Cedar, 1991). The most common example is the silencing of P16 via promoter

hypermethylation, which is found in fifteen percent of PDAC patients (Schutte et al., 1997b). In efforts to identify hypermethylated genes that serve as biomarkers down regulated prior to carcinogenic stages of this disease, nearly one-hundred genes have been identified as potential candidates (G. Li, Ji, Liu, Li, & Zhou, 2012; Omura et al., 2008; A. C. Tan et al., 2009).

The Goggins lab at the Sol Goldman Pancreatic Cancer Research Center is one such lab that has contributed to the identification of hypermethylated biomarkers for PDAC via genome-wide methylation profile (GWMP) (Vincent et al., 2011). In one such study, a GWMP was performed comparing PDAC samples to normal pancreatic tissue. A number of hypermethylated genes were reported common among PDAC samples including: genes in the WNT pathway, adhesion proteins, tumor suppressors, and homeobox transcription factors (Vincent et al., 2011). Another GWMP study performed in conjunction with expression analysis, identified hypermethylated genes present in untreated, resected PDAC tumors compared to matched normal tissue (Nones et al., 2014). While this study reported similar hypermethylated genes as reported by Vincent et al., 2011, genes associated with axonal guidance and pancreatic stellate cell activator proteins were also found to be aberrantly methylated (Nones et al., 2014). While these studies have contributed to our understanding of PDAC etiology, identifying biomarkers specific to each chronological stage of PDAC, such as metastasis, may contribute to therapeutic advancement.

1.5 Metastatic Process in PDAC

As previously mentioned, patients with PDAC have the lowest five-year survival rate amongst all cancer sub-types (Siegel, Ma, Zou, & Jemal, 2014). Poor prognosis is largely due to the fact that at the time of diagnosis, patients manifest advanced staged tumors and subsequently early metastasis, or the dissemination of primary tumors to distal organs (Siegel, Ma, Zou, & Jemal, 2014; Valastyan & Weinberg, 2011). For this reason, understanding the molecular modalities of pancreatic metastasis is critical to advancing therapeutics, and ultimately, to increase patient longevity.

The process of metastasis is a conglomerate of intricate biological steps, as illustrated in Figure 1.4 (Valastyan & Weinberg, 2011). Briefly, pre-invasive cancerous cells must first invade locally, undergo intravasation, survive transmission in circulation, adhere to and extravasate distal parenchyma, survive in secondary environments, and finally colonize in distal organ sites (Valastyan & Weinberg, 2011). Currently, the molecular mechanisms of each sub-process within metastasis are not fully understood; however, prognostic markers for two processes, epithelial-to-mesenchymal transition and the formation of tumor microenvironment, make up the majority of metastatic biomarkers currently used in the diagnosis of PDAC.

In order for metastasis to occur, cancer cells must invade through the basement membrane, of which helps to maintain the polarity and organization of epithelial cells (Ingber, Madri, & Jamieson, 1986; Son & Moon, 2010). In order to invade locally, epithelial cells must lose polarity and adhesion characteristics, to enable the transition into a migratory, mesenchymal-like cell (Mihaljevic, Michalski, Friess, & Kleeff, 2010; Son

& Moon, 2010). This process is called epithelial-to-mesenchymal transition (EMT) and, as previously suggested, is distinguished by the downregulation of epithelial cell markers, and an upregulation of mesenchymal cell markers (Son & Moon, 2010). Our understanding of EMT has led to the identification of a number of metastatic biomarkers (Mihaljevic, Michalski, Friess, & Kleeff, 2010). One such metastatic biomarker, E-cadherin, is a glycoprotein that traverses the membrane of normal epithelium and enables cell-to-cell contact by forming adherens junctions (Shapiro & Weis, 2009). The integrity of these cell-cell junctions is preserved by interactions between the extracellular domains of E-cadherins in adjacent cells, as well as interactions between the intracellular domains of E-cadherins to catenin complexes (Shapiro & Weis, 2009; Tian et al., 2011). A loss of E-cadherin expression is associated with the gain of the mesenchymal cell markers, N-cadherin and vimentin; and thus, an invasive phenotype and poor prognosis among PDAC patients (Nakajima et al., 2004).

Additional biomarkers for PDAC metastasis include growth factors that induce EMT such as TGF- β , hepatocyte growth factor, bone morphogenic protein, and vascular endothelial growth factor (Christofori, 2006; Friess et al., 1993; Itakura et al., 1997; Voorneveld et al., 2013). These growth factors activate expression of transcription factors including SNAIL, TWIST, and ZEB (Son & Moon, 2010). Transcriptional activation from these transcription factors induces changes in gene expression away from epithelial cell markers, in favor of mesenchymal specific genes (Son & Moon, 2010). As previously mentioned, this switch in regulatory molecules promotes EMT, expression of these proteins serve as additional hallmarks of increased cell motility

and metastatic potential of pancreatic tumors (Bronsert et al., 2014; B. Hotz et al., 2007; Lamouille, Xu, & Derynck, 2014; Yin et al., 2007).

Besides EMT, one component recently found to promote the metastasis of PDAC is the interplay between tumor cells and the tumor microenvironment (Feig et al., 2012). Surrounding tumor cells, which make up what is known as the desmoplastic stroma, consist of an extensive extracellular matrix (ECM), as well as inflammatory cells, adipocytes, endothelial cells, and pancreatic stellate cells (Feig et al., 2012). Overall, these cells serve as a barrier between tumor cells and untransformed cells (Bartholin, 2012). Additionally, they serve as targets for adjacent cancer cells, and following activation by cancer cells, can be modulated to create an environment that is advantageous for local invasion (Bartholin, 2012). Specifically, signaling between activated pancreatic stellate cells and cancer cells result in increased ECM deposition, a condition that is referred to as fibrosis (Erkan et al., 2009). This modulation not only results in a decrease of tumor vascularization, but is also one reason that common therapeutic approaches are unsuccessful (Neesse et al., 2011). Expression markers indicative of stromal index and increased invasion are listed below, in Figure 1.5.

While there has been success towards expanding the knowledge of PDAC metastasis, additional molecular mechanisms and prognostic determinants are needed. For this reason, prior work in our lab used a metastatic PDAC cell culture model to understand epigenetically regulated genes that are associated with increased metastatic properties. My project involved validation of specific preliminary results, discussed in

the next chapter, and an attempt to understand the functional relevance of these events as they pertain to the metastasis of PDAC.

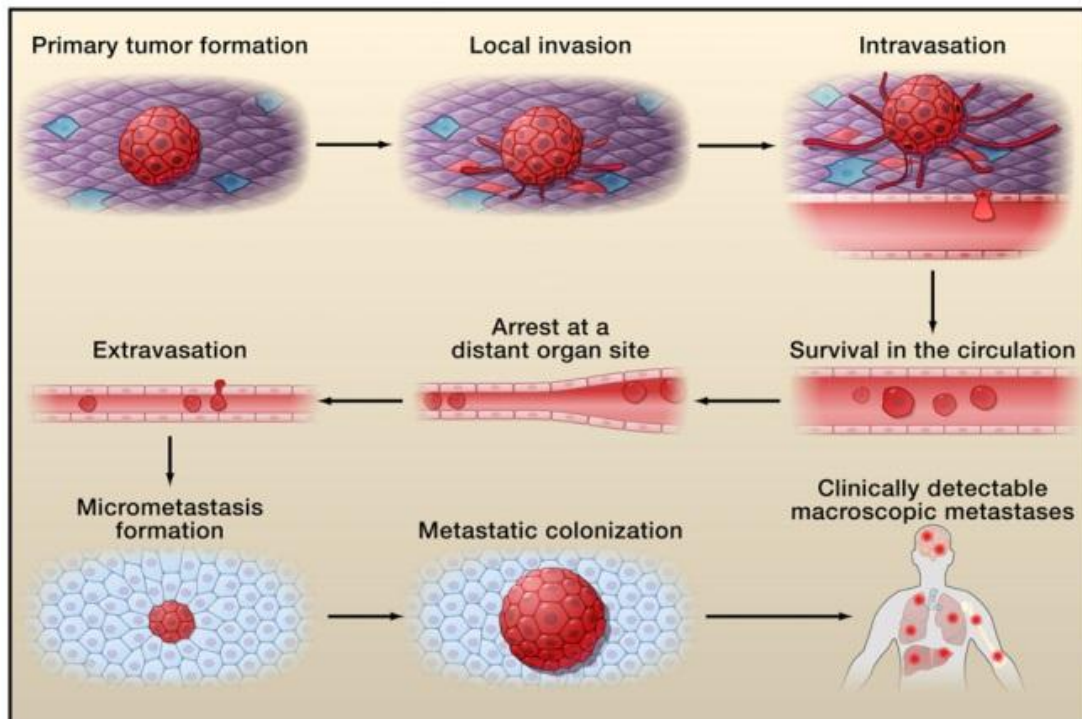


Figure 1.3 Stages of metastasis. In order to travel to distal organs, cancer cells must first invade surrounding tissue. Next, mobile cancer cells invade the basement membrane and intravasate into the bloodstream. If they are able to withstand circulation, they can exit the bloodstream and form metastasis at distal organs (Faltas, 2012). Figure as originally published in Faltas, B. (2012) Cornering metastases: therapeutic targeting of circulating tumor and stem cells. *Front Oncol* 2:68 doi: 10.3389/fonc.2012.00068

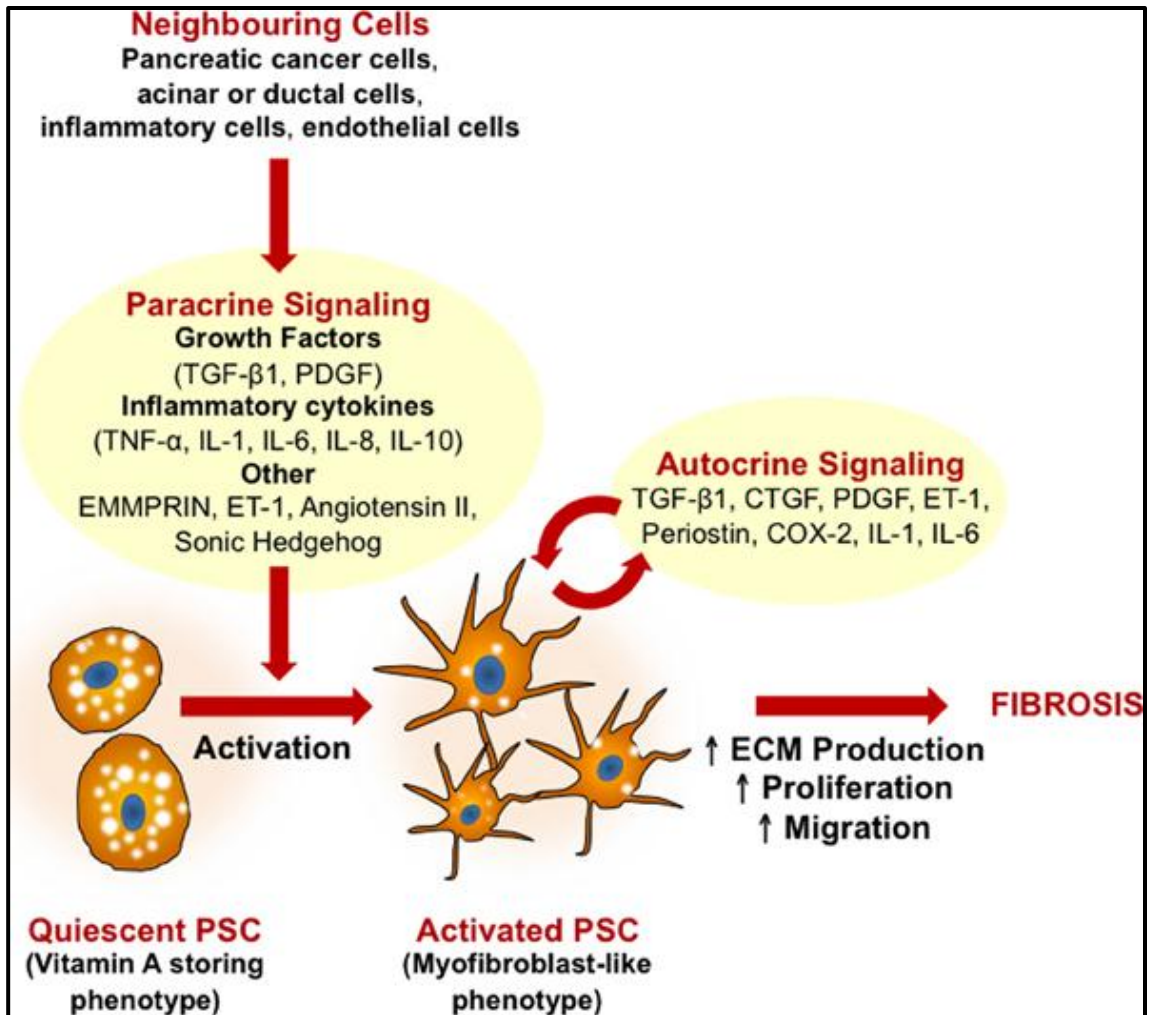


Figure 1.4 Role of tumor microenvironment in PDAC. Cancer cells secrete growth factors and other factors that activate fibroblasts called pancreatic stellate cells (PSC). These PSC then secrete signaling molecules that increase ECM deposition, fibrosis, and ultimately the metastasis of PDAC (McCarroll et al., 2014).
Figure from McCarroll et al., 2014.

Chapter 2

PRELIMINARY WORK

2.1 Genome Wide Methylation Profile

Before explaining preliminary work, I would like to acknowledge Dr. Benjamin Rodriguez and Dr. Zengang Peng, previous lab members in Dr. Huey Jen-Lin's laboratory at Ohio State University, of whom generated this data.

The goal of our laboratory was to identify hypermethylated genes that serve as biomarkers for metastatic PDAC tumors. To identify hypermethylated genes specific to PDAC metastasis, a genome-wide DNA methylation profile (GWMP) was performed using an isogenic metastatic cell culture model, of which consisted of two isogenic variant cell lines (Bruns, Harbison, Kuniyasu, Eue, & Fidler, 1999). The first was generated by orthotopical injection of a cell line established from lymph node metastases, Colo357, in to the spleen of nude mice (R. T. Morgan et al., 1980; Vezeridis et al., 1990). This method induced spontaneous liver metastases in treated animals, and upon isolation in culture, led to the generation of the isogenic metastatic cell line, fast-growing (FG) (Vezeridis et al., 1990). Using the FG cell line, a similar procedure was performed to develop a variant cell line and ultimately a metastatic cell culture model, and is outlined in Figure 2.1 (Bruns, Harbison, Kuniyasu, Eue, & Fidler, 1999). Briefly, orthotopical injections of FG cells were administered into the pancreas of nude mice.

Upon to formation of hepatocyte metastases, metastatic cells were harvested and grown in culture. Following three rounds of orthotopic injections and selection of cells with increased metastatic potential, a highly metastatic isogenic variant of FG cells, designated as L3.6pl, was generated (Bruns, Harbison, Kuniyasu, Eue, & Fidler, 1999).

To characterize the expression profiles of FG compared to L3.6pl, immunohistochemical and situ hybridization were performed (Bruns, Harbison, Kuniyasu, Eue, & Fidler, 1999). These data led to the conclusion that the lowly metastatic variant, FG, expressed epithelial cell markers and lower levels of metastatic biomarkers (Bruns, Harbison, Kuniyasu, Eue, & Fidler, 1999). Conversely, L3.6pl cells exhibited lower levels of epithelial markers and high levels of metastatic biomarkers (Bruns, Harbison, Kuniyasu, Eue, & Fidler, 1999). Additionally, the incidence of spontaneous liver metastasis following intrapancreatic injection was five percent to fifty percent in animals injected with FG to L3.6pl cells, respectively (Bruns, Harbison, Kuniyasu, Eue, & Fidler, 1999). These data suggest that both FG and L3.6pl cell lines may be a useful cell culture model to identify metastatic biomarkers of PDAC.

Using FG and L3.6pl as an *in vivo* metastatic model, previously lab members performed a technique called MBD-isolated Genome Sequencing (MiGS) to identify differential methylation (Serre, Lee, & Ting, 2010). DNA from each isogenic line was fragmented and double stranded DNA containing methylated CpG was bound by GST tagged-methyl-binding domains. Bound DNA was eluted, then underwent massive parallel sequencing and aligned to the human genome (HG18; <http://genome.ucsc.edu>) via the Illumina Genome Analyzer II. Methylation levels were measured by the

proportional abundance of read coverage and the significance of corresponding methylation was determined by Dr. Rodriguez, using the methylation software, MEDIP (Lienhard, Grimm, Morkel, Herwig, & Chavez, 2014). Only CpG islands within the promoter regions of genes, defined as ± 1000 base pairs from transcriptional start sites of a gene, were considered. From this analysis, 38 genes were identified as having at least a five-fold increase of CpG island methylation, and are shown in Figure 2.2.

2.2 ZNF300 as a Candidate Hypermethylated Gene

Out of the 38 hypermethylated gene candidates, genes whose role in cancer had yet to be elucidated were considered for further validation. A semi-quantitative methylation technique known as Combined Bisulfite Restriction Analysis (COBRA), described in the method section, was used to validate CpG island (CGI) methylation. In addition to validating CGI methylation of each target gene, genes that exhibited methylation in PDAC lines compared to non-malignant pancreatic cell lines were chosen as future candidate genes. Figure 2.3 depicts COBRA results, which confirmed differential methylation within a novel gene, Zinc Finger Protein 300 (ZNF300), between FG and L3.6pl. More importantly, ZNF300 was one of the few genes found to be non-methylated in non-malignant, pancreatic cell lines. Because the ZNF300 CGI appeared to be methylated in only PDAC cell lines, this gene was chosen as a candidate biomarker gene for PDAC.

While the COBRA results suggested ZNF300 may be hypermethylated in the highly metastatic L3.6pl cell line, this method only detects methylation of specific

CpG dinucleotides, rather than overall CGI methylation. To accurately quantify the overall ZNF300 CGI methylation, pyrosequencing was performed in both FG and L3.6pl cells. Pyrosequencing results, shown in Figure 2.4, indicate an overall fifteen percent increase of ZNF300 CGI methylation in L3.6pl compared to FG. In order to identify the regulatory regions of the ZNF300, a Luciferase reporter assay was performed. Target regions used in the reporter assay included the ZNF300 CpG island and the flanking promoter sequences. Results from this study led to the conclusion that the transcriptional activity was the greatest when the ZNF300 CGI was present, as measured by the Luciferase activity, and is shown in Figure 2.4. Taken together, the promoter assay data and validation of methylation within the ZNF300 CGI suggested that ZNF300 may be an epigenetically regulated gene.

To determine the clinical significance of ZNF300 expression, previous lab members performed immunohistochemical staining using paraffin-embedded sections from benign, primary pancreatic tumors, and metastatic lymph nodes. Figure 2.5 shows one of the ten samples from PDAC patients, and indicates ZNF300 expression in both benign and primary pancreatic tumor sections collected from PDAC patients. Interestingly, in the lymph node metastases section, ZNF300 expression appears to decrease. ZNF300 expression was decreased compared to the primary pancreatic tumor in approximately all ten patient samples. Collectively, these data suggest that ZNF300 may be a clinically relevant gene in the metastasis of PDAC.

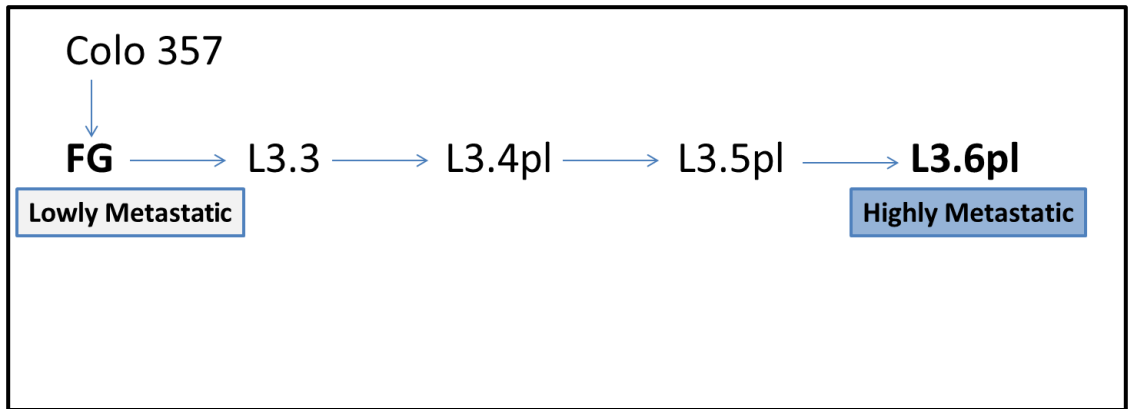


Figure 2.1 Schematic of FG and L3.6pl cell line generation used in GWMP. Briefly, Colo357 cells established from metastatic lymph nodes by Morgan et al. were orthotopically injected into the spleen of mice whereby the fast-growing cells (FG) were selected in culture as described in Vezeridis et al. to yield the lowly metastatic variant used in the GWMP. The highly metastatic variant used in the GWMP, L3.6pl, was generated via Bruns et al., using orthotopic injections in the spleen of nude mice, and following spontaneous formation of liver metastasis, were isolated and propagated in culture to generate L3.3. To select for cells with enhanced metastatic ability in pancreatic tissue, L3.3 cells were injected three independent times into the pancreas of nude mice, whereby metastatic cells of spontaneous liver metastasis were harvested and cultured. (Bruns, Harbison, Kuniyasu, Eue, & Fidler, 1999; R. T. Morgan et al., 1980; Vezeridis et al., 1990)

Genes of Interest	Non-Malignant Pancreatic Cell Lines		Pancreatic Cancer Cell Lines							
	HPDE	HPNE	Colo357	FG	L3.6pl	BXPC3	HS766T	Miapaca2	Panc03.27	Panc1
COL7A1		hyper			hyper			hyper		
FOXL1	Hyper				hyper			hyper		
HNF1B		hyper			hyper	hyper	hyper	hyper		hyper
NID2	Hyper				hyper	hyper	hyper	hyper	hyper	hyper
PTK6		hyper			hyper			hyper		
TPM2					hyper					
ZNF300					hyper				hyper	hyper

Figure 2.2 CGI methylation in non-malignant and PDAC cell lines as indicated by COBRA. ZNF300, shown at the bottom, was chosen as the candidate gene of interest due to the presence of CGI methylation in multiple PDAC lines while remaining non-methylated in non-malignant pancreatic cell lines. (Figure adapted from preliminary work by Dr. Zhengang Peng)

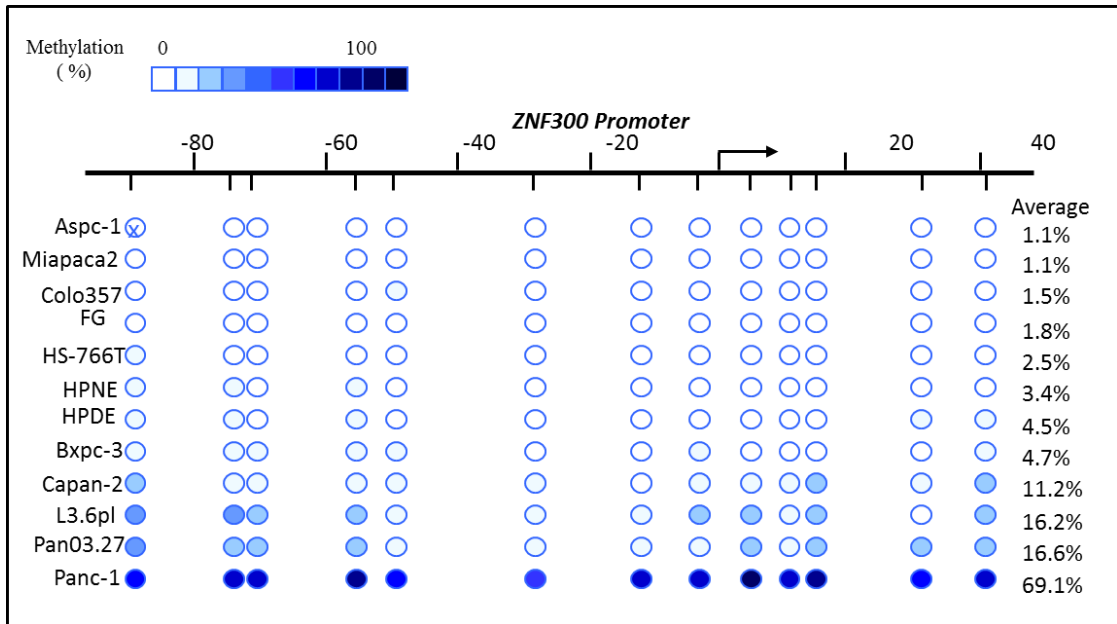


Figure 2.3 Overall methylation of the ZNF300 CGI in PDAC lines. Pyrosequencing results indicate that L3.6pl exhibits increased ZNF300 CGI methylation relative to FG, and many others. (Figured adapted from preliminary work by Dr. Zhengang Peng)

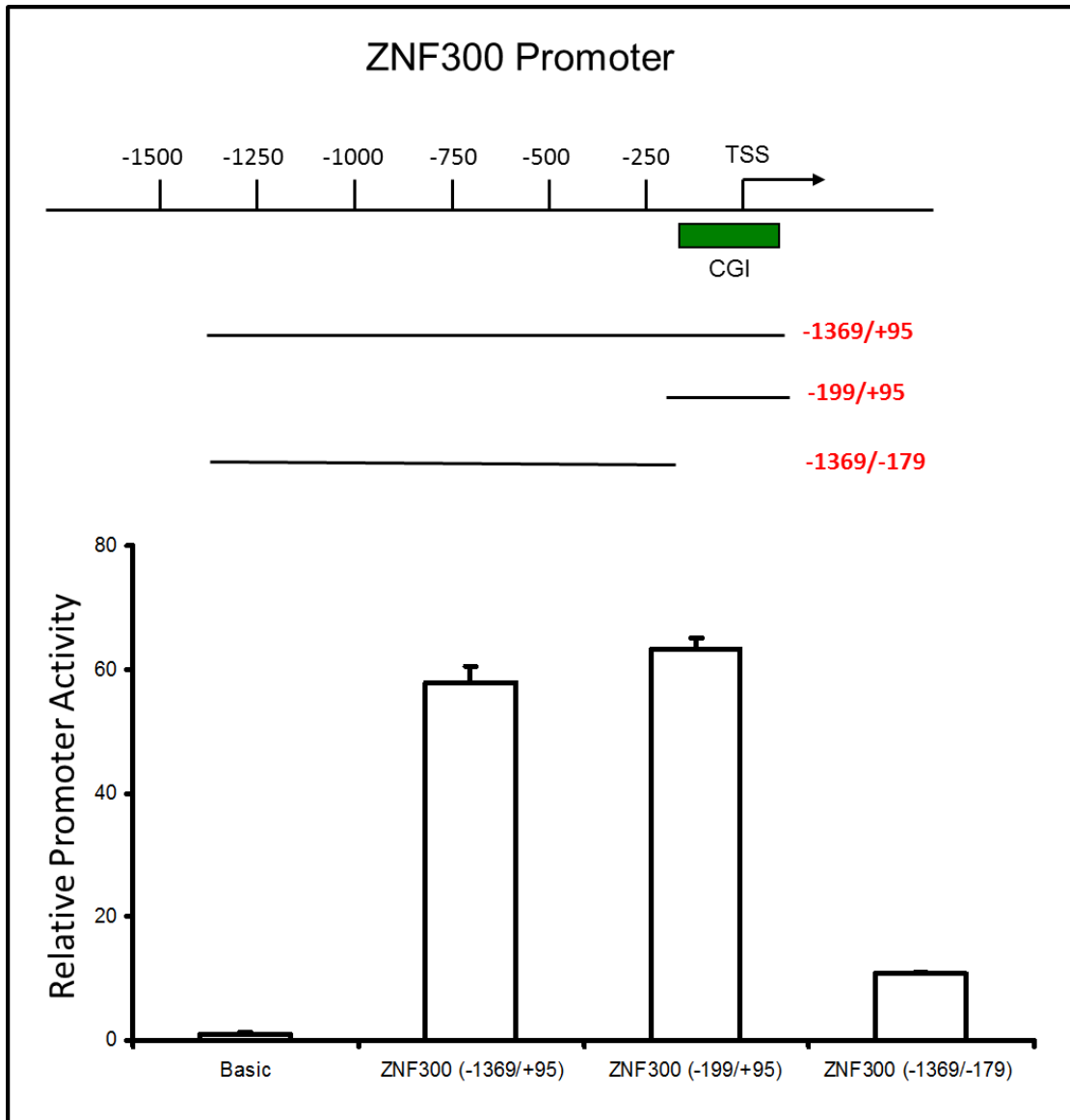


Figure 2.4 Luciferase reporter assay under the ZNF300 promoter. Results from reporter assays show that the transcriptional activity driven under the ZNF300 CGI (-199/+95) induces luciferase activity comparable to the entire cloned region, (-1369/+95). Conversely, Luciferase activity is attenuated when the ZNF300 CGI is not included, (-199/+95). (Figured adapted from preliminary work by Dr. Zhengang Peng)

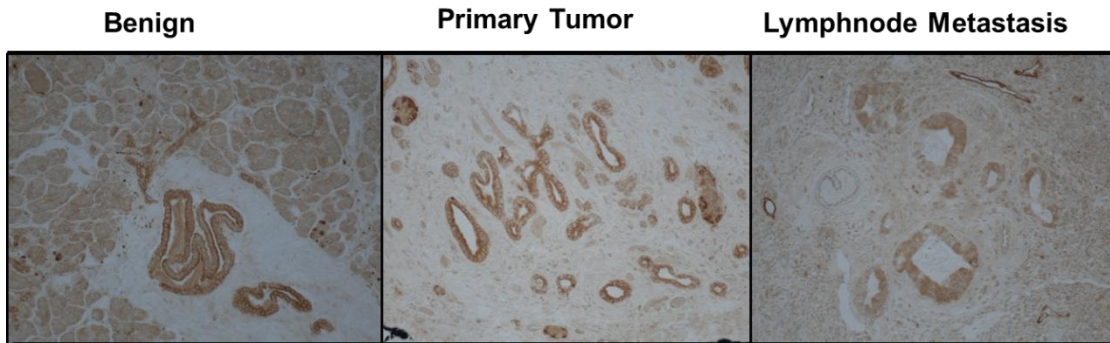


Figure 2.5 Immunohistochemical staining of ZNF300 in paraffin-embedded patient tissues. In benign primary tumor pancreatic sections, ZNF300 expression is apparent; however, in metastatic lesions from the same patient ZNF300 expression is decreased.

2.3 Hypothesis

Preliminary data using a metastatic *in vivo* cell culture model has led to our hypothesis that ZNF300 may be an epigenetically regulated, candidate biomarker for PDAC metastasis. To determine ZNF300 methylation differences between metastatic cell lines, my first aim was to measure the correlation between ZNF300 methylation and expression of ZNF300 over time in culture. Following validation, the second aim was focused on elucidating the functional role ZNF300 may have in the metastatic process within PDAC.

Chapter 3

METHODS AND MATERIALS

3.1 Cell Culture

PDAC cell lines: Colo357, L3.6pl, FG, and Panc1 were purchased from the Fidler Lab (University of Texas MD Anderson Cancer Center, Houston, TX). Cells were grown in conditions as suggested by the distributor: 1XDMEM (Fisher Scientific™, Cat.No. MT10017cvrf, Pittsburg, PA) supplemented with 10% FBS (Gibco®, Cat. No. 26140, Grand Island, NY) 1% AA (Gibco®, Cat. No. 15240-062, Grand Island, NY) and 1X NEAA (Gibco®, Cat. No. 111040-050, Grand Island, NY) were used as media for cell lines. Cells were grown at 37⁰C with 5% CO₂. Cell lines were thawed from liquid nitrogen and allowed to grow for 1 week prior to use for experiments. Upon reaching 60-80% confluency, 0.05% trypsin (Gibco®, Cat. No. 25300-054, Grand Island, NY) was used to detach cells from 10cm² dishes. Cells were pelleted via centrifugation at 1000rpms for five minutes. The supernatant containing trypsin was removed and cells were resuspended in maintenance media as described above. A 1:10 dilution of cells were seeded in a final volume of roughly 8mls of maintenance media. Cells were only used at passage 3 or 4 for experiments; this corresponds to roughly 1.5 to 2.5 weeks in culture.

3.2 Protein Isolation

To isolate protein, cell pellets were rinsed two times with PBS before protein was extracted. Cell pellets were put on ice whereby 45ul of 1X Ripa Buffer (Cell Signaling Technology, Cat. No. 50-195-822, Beverly, MA,) was used in junction with 2.5ul of 1x Protease Inhibitor Cocktail (Roche, Cat. No. 04693159001, Indianapolis, IN). To each sample, the pellet was homogenized with an Eppendorf tube pestle using 45 strokes, then put back on ice for 45 minutes. Following incubation on ice, samples were spun for 15 minutes at 15000xg. The supernatant was then collected and stored at -80°C if not immediately used in western blotting applications.

3.3 Western Blotting

To quantify the protein concentration of each sample, the Bio-Rad Protein Assay colorimetric dye (Bio-Rad, Cat. N0. 500-0006, Hercules, CA) was used. The dye was used at a 1:5 dilution with autoclaved water. Each protein sample was diluted 1:7 for accurate quantification of highly concentrated samples. 2ul of diluted protein samples was added to 200ul of diluted dye. After 5 minutes the absorbance was measured using 560nm wavelength on the Glomax® Detection System(Promega, Cat.No. 8032, Madison, WI). Absorbance was used to calculate protein concentration via a standard curve using 10mg/ml, 5mg/ml, 2.5mg/ml, 1.25mg/ml, 0.625mg/ml, and 0.31mg/ml. Each standard was also diluted at 1:7 for accurate quantification so ensure quantification was determined in the linear range of the spectrophotometer. Once protein concentration was calculated, 40ug of protein was diluted with 2x laemmli

buffer (1M dithiothreitol (DTT), 1% bromophenol blue, 10% SDS, and 1M Tris-CL pH of 6.8) to a final concentration of 1x to ensure equal volume between samples. Samples were loaded on 4-15% Mini-PROTEAN® precast gel(Bio-Rad, Cat.No. 456-1084, Madison, WI) and ran at 100volts for 120 minutes for cell passage experiments. For time course experiments 4-20% Tris-HEPES-Gycline precast gels (ThermoScientific™, Cat. No. 456-1084, Waltham, MA) were used along with the recommended 1x Tris-HEPES-Glycine buffer (1X buffer is 100mM Tris, 100mM HEPES, 0.1% SDS, pH 8.0). To transfer, methanol activated PVDF membrane (GE™) was immersed in 1xTransfer Buffer (2L, 25 mM Tris, 192 mM glycine, 10% methanol). Protein transfers were ran at 75volts for 90 minutes on ice. Membranes were stained with Ponceau (0.1% (x/v) Ponceau S in 1% (v/v) acetic acid) for five minutes to verify protein had successfully transferred. Membranes were then rinsed with ddH₂O three times, destained with 0.1%NaOH for two minutes, and rinsed for five minutes with ddH₂O at room temperature. Next, membranes were blocked in TBS (20mM Tris and 150 mM NaCl) buffer containing 0.1% tween-20 and 5% milk powder for one hour. Primary antibodies, were diluted in blocking buffer and incubated over night at 4^oC. Blots were brought to room temperature and rinsed three times, 20 minutes each with TBS-t with 0.1% tween 20. Secondary antibody, Goat Anti-Rabbit HRP conjugate (BioRad, Cat. No. 170-6515, Madison, WI) was used at a 1:3000 dilution in blocking buffer for 60 minute incubations at room temperature. Membranes were then rinsed with TBS-t 0.1% tween-20 three time for twenty minutes then developed using ECL (Thermo Scientific™, Peirce™, Cat. No. 32109, Waltham,

MA) at the recommended 1:1 ratio. Autoradiography film (Thermo Scientific™, Cat. No. 34090, Waltham, MA) was used for chemiluminescence detection.

Table 3.1 Antibodies utilized to detect protein expression

Antibody	Isotype	Production	Dilution	Distributor	Catalog Number
Anti-Human ZNF300	Rabbit IgG	Polyclonal	1:500	Abbiotec	650641
Anti-Human β -Actin	Rabbit IgG	Monoclonal	1:1000	Cell Signaling	13E5, 5125s

3.4 RNA Isolation

Cells were harvested using the TRIzol® Reagent (Ambion-Life Technologies, Cat. No.15596-026, Carlsbad, California) per the distributors suggestion. To every 1ml TRIzol® collected, 200ul of chloroform was used followed by a vigorous vortex and incubation at room temperature for 2-3 minutes. Next, centrifugation at 12,000xg was done at 2-8⁰C for 15 minutes. The top clear layer containing the RNA was collected and 500ul of isopropyl alcohol was added to precipitate the RNA out of solution. After a10 minute incubation at room temperature, a centrifugation step was performed at 12,000xg for 10 minutes. Once the pellet was located, the supernatant was removed and the pellet was washed in 1ml of 75% ethanol then centrifuged at 12,000xg for 5 minutes. Upon removal of the supernatant, the pellet was allowed to

dry then 20ul of RNase free H₂O was used to dissolve the pellet. RNA was then incubated at 65⁰C for 10 minutes and stored at -80⁰C.

3.5 cDNA Synthesis

Approximately 1µg of RNA was used as template in reverse transcription experiments. RNA quantitation was determined using the NanoDrop 2000 (Thermo Scientific™, Cat.No. Waltham, MA). Prior to the generation of cDNA, DNase treatment was performed using DNase I Amp Grade (Invitrogen™, Cat. No. 18068-015, Grand Island, NY). To do this, 1µg of RNA was used in conjunction with 1µl of 10X DNase I Reaction Buffer, 1µl of DNase I enzyme, and then brought to 10ul total volume with nuclease free water. The reaction was incubated at room temperature for 15 minutes, and stopped using 1 µl of 25 mM EDTA solution supplied by Invitrogen, and incubated at 65⁰C for 10 minutes, then ready for reverse transcription(RT). RT cocktails consisted of the following 5µl of 10µM oligo dT, 0.4µl of 25mM dNTP, and 1µg of DNase treated RNA. Samples were then incubated at 65⁰C for five minutes followed by one minute on ice. Next 4µl of 5X Buffer, 1µl of 0.1M DTT, 1µl of RNase Inhibitor, and 1.2µl of Superscript III (Invitrogen™, Cat. No. 1502358, Grand Island, NY) were added and cycled at 50⁰C for 50 minutes, 70⁰C for 15 minutes, and 4⁰C no more than 12 hours. Following RT, samples were diluted 1:10 with molecular grade H₂O and stored at -20⁰C until further use.

3.6 Quantitative Reverse Transcription Polymerase Chain Reaction

Quantitative reverse transcription polymerase chain reaction (qRT-PCR) applications were carried out using 10 μ l of HotStart-IT Syber Green qPCR Master Mix(2X) (Affymetrix®, Cat.No. 75762, Santa Clara, CA), 0.4 μ l ROX™, 4 μ l of 1:10 diluted cDNA, 1 μ l of 5 μ M primers shown in Table 3.2, and ddH₂O to a total volume of 20 μ l. The 7500 ABI Fast Real Time PCR System was used to cycle at the following conditions: 1 x at 95⁰C for 2 minutes to denature the primer quenching protein, then 45x at [95⁰C for 5 seconds, 56⁰C for 30seconds, and 72⁰C for 2 minutes]. Data was exported as C_T values; a value that is determined by the point at which the threshold of fluorescence emission and amplification plot of each target intersects. C_T values are inversely related to transcript levels; thus, more abundant cDNAs reach the threshold value before less abundant cDNAs, yielding higher C_T values. To determine target transcript levels, each C_T value was normalized to C_T value of β -Actin, which served as the housekeeping gene. The following calculations were used to ultimately yield relative target transcript levels:

- I. $\Delta C_T = C_{TX} - C_{TR}$ (the difference in threshold cycles for target and reference)
- II. $\Delta\Delta C_T = \Delta C_{TX} - \Delta C_{TR}$ (the difference of ΔC_T for each treated sample to control)
- III. $2^{(-\Delta\Delta C_T)}$

Table 3.2 Primer sequences used in qRT-PCR

Transcript Target	Primer Sequence
ZNF300	Forward: 5'GGTCTCAATGGGGTATCCAGT 3' Reverse: 5' TTCTTCCCTTGTCTCCCATCT 3'
B-Actin	Forward: 5'CAT CCT CAC CCT GAA GTA CCC 3' Reverse: 5'AGC CTG GAT AGC AAC GTA CAT G 3'

3.7 DNA Isolation

DNA was isolated from frozen cell pellets that had been stored at -80°C . The Qiagen QIAamp® DNA Mini Kit (Qiagen®, Cat.No.51304,Valencia, CA) was used to isolated DNA following the Blood and Body Fluid Protocol. 20µl of Qiagen Proteinase K was added to a 1.5ml microcentrifuge tube. Cells were resuspended in 200µl fresh 1X PBS buffer, then added to the microcentrifuge tube. Next, 200µl Buffer AL was added and the sample was vortexed for 15 seconds to ensure homogeneity. The samples were incubated for 15 minutes at 56°C for maximal lysis. Following the addition of 200µl of 100% ethanol and a 15 second vortex, samples were then loaded onto QIAamp Spin Columns and spun at 6800xg for 1 minute. Flow through was removed and 500µl of wash buffers AW1 and AW2 were added independently then spun at 6800xg for 1 minute each. Once washes were completed a final spin was completed to dry the column. 200µl of molecular grade water was used

to elute DNA via final spin at 6800xg for 1 minute. DNA was stored at -20°C until further use.

3.8 Bisulfite Conversion

Bisulfite conversion was performed using the EZ DNA Methylation-Lightning™ Kit (Zymo Research, Irvine, CA. Cat.No.D5030, Irvine, CA). 350ng was used in all bisulfite conversions, the median suggested by the manufacturer. DNA was brought to a total volume of 20µl with molecular grade water whereby 130µl of Lightning Conversion Reagent was added to each bisulfite reaction. Samples were incubated at 98°C for 8 minutes, 56°C for 60 minutes, and then held at 4°C for no more than 24 hours. To desulphonate samples, 600µl of binding buffer and the sample were added to a spin column and spun at 15,000x g for 30 seconds. Two washes consisting of 200µl of ethanol were used to clean DNA bound on the column followed by a 1 minute spin at 12,000x g. Samples were eluted with 10ul of ddH₂O and stored at -20°C for no more than one month.

3.9 Bisulfite Converted Polymerase Chain Reaction

In amplifying CpG islands in the promoters regions of ZNF300, Go Taq®Hotstart Green Master Mix 2X (Promega™, Cat. No.M5123, Madison, WI) was used which contained: 400µM dATP, 400µM dGTP, 400µM dCTP, 400µM dTTP and 4mM MgCl. All primers are shown in Table 3.3 and were designed by Methyl Primer Express® Software v1.0 (Applied Biosystems®, Grand Island, NY) to minimize the

bias amplification of either methylated or unmethylated DNA. The sequence of the CGI was obtained by the UCSC Genome Browser available online and is shown in Table 3.3. Due to the size limitations of polymerase chain reaction (PCR) products generated from bisulfite converted DNA, only 209bp out the total 250bp was subject to amplification. Products were ran on a 1% agarose gel in 1x TBE using gel electrophoresis to ensure proper amplicon length of 209bp.

Table 3.3 COBRA primers for ZNF300 CGI

Genomic Target	Primer Sequence
ZNF300 CGI	Forward: 5'TTA GAG GTT TTG TTT AGG AAG TAA TAT G 3' Reverse::5'ACA AAA ATA TAC TCC TTA ATA CTC CTT TC 3'

3.10 Combined Bisulfite Restriction Enzyme Analysis (COBRA)

DNA samples were first bisulfite converted, then the ZNF300 CGI was PCR amplified as described above. Each reaction was purified using the MiniElute PCR Purification Kit (Qiagen®, Cat. No. 28006, Valencia, CA). First five volumes of Buffer PB was mixed with each reaction then added to the MiniElute Spin Column. Samples were centrifuged at 15,000xg for 1 minute and flow-through was discarded. Next, 750µl of Buffer PE was used to wash the column, then spun again at 12,000rpm

for one minute. Columns were centrifuged for an additional spin to dry the columns, then 10µl of DNase-free water was used to elute the DNA per manufactures instructions. To each reaction, 0.5µl of AciI restriction enzyme was added and incubated at 37⁰C for approximately 150 minutes then ran on a 10% polyacrylamide precast gel (Invitrogen™, EC2275, Grand Island, NY) using 1x TBE for four hours at 50 volts. The gel was then stained with 0.1% ethidium bromide then imaged (Foto/Analyst® MiniVisionary Systems, Cat. No.60-2030, Hartland, WI). The AciI cut sequence is 5' CCGC 3'; possible cut sites of retained CpG dinucleotides within the ZNF300 CGI are shown in Figure 3.1. The positive control consisted of universally methylated DNA (Promega, Cat.No.1231, Madison, WI) which was bisulfite converted and then used in PCR to amplify the ZNF300 CGI, as described in previous sections. Gel electrophoresis and DNA purification was also performed whereby the entire process was repeated again to yield the negative control. The positive and negative controls were then used in COBRA procedures, as described above.

ZNF300 CGI Sequence:

```
TtagaggttttgtttaggaagtaatatggtgtttttggagttgttttCGtatggggtCGttatTTTgagagttC
      ↓                                     ↓
GGtCGttttCGtattagCGgaggattCGtttagtgttgagttCGagaatggggtgtattatagCGgtagCG
aaggagggggaaggCGaCGgaaaggaggttgCGaaaggagtattaaggagtatattttgt
```

Figure 3.1 The ZNF300 CGI forward sequence. Upon bisulfite conversion and PCR amplification, AciI digests results in two fragments in the first amplicon, and three in the second. The ZNF300 CGI amplicon (209bp out of 250bp) is represented in black, and the flanking regions which consist of primers are gray. All primers are highlighted in gray.

3.11 Transformations of Bisulfite-PCR

Once PCR products were generated and validated using agarose gel electrophoresis, 0.5ul of each sample was used to clone fragments into Topo®TA Cloning Kit® (Invitrogen™, Cat. No. 450-Carlsbad, CA.) Specifically reactions consisted of: 1ul of Salt Solution, 1µl of Topo®TA vector, and molecular grade water up to 6ul total volume. A positive PCR reaction supplied with the kit and vector-only controls were performed in tandem as controls. Samples were incubated at room temperature for 30 minutes and 2µl of each reaction was added to 30ul of DH5α-Max Efficiency competent cells (Invitrogen™, Cat.No.18258-012, Carlsbad, CA). Transformations were carried out via incubations in ice-water baths for 30 minutes followed by a 45 second heat shock at 42⁰C, then 2 minutes on ice. 500µl of S.O.C. media provided was added to each transformation and incubated at 37⁰C while

shaking at 200RPM for 1 hour. Next, samples were spun at 3,900rpm for 10 minutes to pellet the bacteria. The supernatant was removed and the pellet was resuspended in 60µl of fresh S.O.C. Last, 50µl of each sample was plated on LB agar (Fisher BioReagents®, Cat. No. 9724-500, Pittsburg, PA) plates containing 1x ampicillin(Fisher BioReagents®, Cat. No. BP 1760-5, Pittsburg PA) and 40mg/ml of β-galactosidase (ThermoScientific™, Cat. No. R0401, Waltham, MA) and allowed to grow for 24 hours at 37°C. If colonies were present, they were individually picked and cultures were grown using LB broth (Fisher BioReagents®, Cat. No. BP 1426-500, Pittsburg, PA) with 1x ampicillin overnight at 37°C and shook at 200rpm. Once the cultures had grown for 18 hours the bacteria was pelleted via a spin at 3,500xg for 10 minutes. Once the supernatant was removed, pellets were froze for up to 24 hours, or used immediately in mini prep procedures.

3.12 Mini Preps

To isolate plasmid DNA, mini preps were performed using the Wizard®Plus SV Mini Prep Kit(Promega, Cat. No.A1330, Madison, WI). First the pellets were resuspended in 250µl of Cell Resuspension Solution, then 250µl of Cell Lysis Buffer followed 4-6 inversions to ensure homogeneity. Next, 10µl of Alkaline Protease Solution followed by 350µl of Neutralization Buffer was added to each sample. Samples were then centrifuged at max speed for 10 minutes. The supernatant containing the plasmid DNA was then transferred to a spin column and centrifuged at 15,000xg for one minute. The flow through was discarded and the column was washed

2x using 750µl of Wash Solution each time following a one minute spin at 15,000xg. Once the column containing the plasmid DNA was washed, a separate spin was performed to dry the column. Last, the DNA was eluted using 100µl of nuclease-free water with a final spin at 15,000xg for one minute. DNA was stored at -20°C until sent for sequencing at University of Delaware DNA Sequencing & Genotyping Center at Delaware Biotechnology Institute. Approximately 10µl of DNA (50-75ng/µl) was sent for sequencing. Primers utilized for sequencing are listed in Table 3.4.

Table 3.4 Sequencing primers for Topo®TA vector

Genomic Target	Primer Sequence
TopoTA Vector	M13 Forward: 5' GTA AAA CGA CGG CCA GT 3'

3.13 Retroviral Infections

For retroviral delivery and expression of ZNF300, the p-RetroX™-TetOn® Inducible Expression System (CloneTech™, Cat. No. 631188, Mountainview, CA). As suggested by manufacturer, all cell lines were given medium containing TET-free FBS (CloneTech™, Cat. No. 631106, Mountainview, CA). Briefly, L3.6pl cells with stably integrated p-RetroX-Tet3 were provided courtesy of Dr. Huey Jen Lee Lin. To infect these cells, viral particles were packaged via G2-293 Packing Cells provided with the infection kit. First, G2-293 cells were seeded at 1.5×10^6 in 1XDMEM

(Fisher Scientific™, Cat. No. 10-013-CV, Pittsburg, PA) in 60mm culture dishes. 24 hours later both the envelope vector, pAmpho, and p-RetroX-Tre3G-ZNF300 (synthesized by GeneArt®, Invitrogen, Carlsbad, CA) or p-RetroX-TRE3G-Luc positive control provided in the kit were delivered via transfection reagent X-fect (CloneTech™, Cat. No. 631317, Mountainview, CA). In tube 1, 5µg of each the envelope vector and p-RetroX-TRE3G-ZNF300 along with X-fect Reaction Buffer to a total volume of 220µl were vortex together and spun down briefly. Next, 3µl of X-fect Polymer was mixed with 217µl of X-fect Reaction Buffer, vortexed, then spun down briefly. Tube 2 was then added to Tube 1, vortexed, and spun down followed by 10 minute incubation at room temperature. The reaction was then added to the G2-293 cells and placed at 37⁰C at 5% CO₂ for 10 hours before media was changed. Next, L3.6pl-Tet cells were seeded at 8 x 10⁵ 24 in 60mm culture dishes prior to infection in maintenance medium. 48 hours post transfection of packaging and target DNA to G2-293 cells, viral particles were collected and G2-293 were given additional media. Approximately one third of the total volume in L3.6pl-Tet dishes, roughly 300µl, was the amount of pRetroX-TRE3G-ZNF300 viral particles or control particles used to infect L3.6pl-Tet cells. Infections lasted 8 hours and following media changes, 12 hours were given to infected L3.6pl-Tet cells to allow for recovery and buildup of Tet-On-3G activator protein. 20 hours post infection, 800ng/ml of doxycycline was used to induce L3.6pl-Tet-ZNF300, L3.6pl-Tet-EV, L3.6pl-Tet-Luc, and L3.6pl-Tet cells. At 3, 6, 12, 24 hours post infect L3.6pl-Tet containing various vectors under the conditions plus and minus doxycycline were trypsinized as described above. Pellets

were collected and stored at -80°C for protein and RNA analysis as described in sections 3.2 and 3.4 respectively.

3.14 Transwell Migration Assay

Migration assays were performed using transparent PET membranes, 24-well 8 μm pore size (BD falcon, REF353097, San Jose, CA). L3.6pl cells were sat at 1.5×10^4 density and FG cells were sat at 1×10^6 in 200ul medium containing no FBS. Chambers were immersed in 500ul of maintenance medium containing normal amounts of FBS for chemoattraction for 24 hours at 37°C , 5% CO_2 to allow for migration. Following incubation, chambers were removed from the wells and the cells that failed to migrate were removed with cotton swabs. Next, migratory cells were fixed with 70% ethanol for 10 minutes, stained with 0.5% cresyl violet for 30 minutes, and rinsed three times with PBS. Membranes were mounted onto cover slips with PBS, and the cells per field of ten images were counted at 100x magnification using an inverted light microscope.

Chapter 4

RESULTS

4.1 Validation of Methylation within the CpG Island of ZNF300

To verify DNA methylation within the ZNF300 CGI of FG and L3.6pl cell lines, I used a method called Combined Bisulfite Restriction Analysis (COBRA). This procedure enabled the visualization of differential ZNF CGI methylation, and is outlined in Figure 4.1. In this technique, genomic DNA was bisulfite converted whereby unmethylated cytosine (C) nucleotides were converted to uracil (U); conversely, methylated cytosines (^{5m}C) were retained (Xiong & Laird, 1997). Next, a region of the ZNF300 CGI was targeted via bisulfite-specific primers, and amplified via PCR to yield an amplicon of approximately 209 base pairs. At this step, (^{5m}C) residues were maintained as C nucleotides and bisulfite converted U nucleotides were replaced with thymine (T) (Xiong & Laird, 1997). Due to contingencies when amplifying methylated DNA, only 209 out of 250 base pairs of the ZNF300 CGI were subject to amplification. ZNF300 CGI methylation was determined by restriction enzyme digestion using *AciI*, an enzyme that cleaves the methylation dependent sequence 5'C⁺CGC 3', then visualized by gel electrophoresis applications. By using a restriction enzyme with C nucleotides, only methylated CpG dinucleotides were subject to digestion; conversely, unmethylated template resulted in the sequence

5'TTGT 3', and therefore was not targeted by *AciI* digestion. Figure 4.1 shows the differential ZNF300 CGI methylation in FG and L3.6pl cell lines following COBRA. The observed fragmented DNA suggests that both the universally methylated DNA, serving as the positive control, and DNA from L3.6pl cells exhibited methylation at the respective CpG dinucleotides. Both FG and the universally unmethylated DNA, serving as the negative control, did not exhibit fragmentation, and therefore exhibited non-methylation at the targeted CpG dinucleotides within the ZNF300 CGI.

To ascertain potential changes in ZNF300 CGI methylation over time in culture, DNA from FG and L3.6pl cell lines was collected over increasing passages and analyzed via COBRA. Figure 4.2 reflects a positive correlation between ZNF300 CGI methylation and time in culture in both FG and L3.6pl cell lines. Specifically, DNA from FG cells at passage two and three exhibited no apparent digestion of the ZNF300 CGI amplicon, indicating a lack of methylation at the respective CpG dinucleotides; however, as passage number increases, the ZNF300 CGI gains methylation at the respective CpGs, as indicated by the presence of fragmentation. A similar trend is reflected in L3.6pl cells; while methylation was apparent beginning at passage two, there was also an increase in methylation over time in culture. These results confirm that culture conditions do affect ZNF300 CGI methylation; therefore future experiments were performed at passage three to circumvent cell culture effects.

COBRA applications successfully identified DNA methylation patterns at specific CpG dinucleotides within the ZNF300 CGI; however, to elucidate overall methylation patterns, bisulfite sequencing was performed. Once again, due to

contingencies when amplifying methylated DNA, only 209 out of 250 base pairs of the ZNF300 CGI were subject to amplification and sequencing. DNA, from cell passages three and four, was isolated from each cell line and used in bisulfite sequencing. Figure 4.3 represents the methylation status at each of the 13 CpG dinucleotides within the ZNF300 CGI of FG and L3.6pl DNA. As seen in COBRA analysis, bisulfite sequencing results also suggest that methylation patterns within the ZNF300 CGI change over passage in culture, in both FG and L3.6pl. These data were used to generate the averaged, total ZNF300 CGI methylation in each sample, and is shown in Figure 4.4. At passage three, the overall ZNF300 CGI methylation appeared higher in L3.6pl cells compared to FG; however, this difference did not reach significance. Similarly, in passage four, ZNF300 CGI methylation levels increased in FG cells, but remain comparable to L3.6pl. In summary, while the methylation of individual CpG dinucleotides within the ZNF300 CGI changed over time in both cell lines, these changes did not result in a significant overall difference.

4.2 Correlation of ZNF300 Methylation and Expression

The second goal of my first aim was to ascertain whether methylation levels correlate to ZNF300 expression. To quantify ZNF300 transcript levels in both FG and L3.6pl cell lines with increasing cell passage, qRT-PCR was performed. Results, shown in Figure 4.5, suggest a potential difference in transcript levels between FG and L3.6pl at passages 4 and 5; however, more replications using additional biological replicates are needed to confirm statistical significance. To determine ZNF300 protein

expression in both cell lines, western blotting was performed, and are shown in Figure 4.6. Western blotting results suggested two things: first, they illustrate that there is no difference in ZNF300 expression between FG and L3.6pl cells at either cell passage. Additionally, ZNF300 expression remained stagnant across cell passage, for each cell line. To show the relationship between methylation and expression, the averaged expression and methylation values are plotted in Figure 4.7. Just as these independent variables were not found to be significant in each study, there was no association found between ZNF300 expression and methylation in both FG and L3.6pl according to a Pearson's correlation analysis.

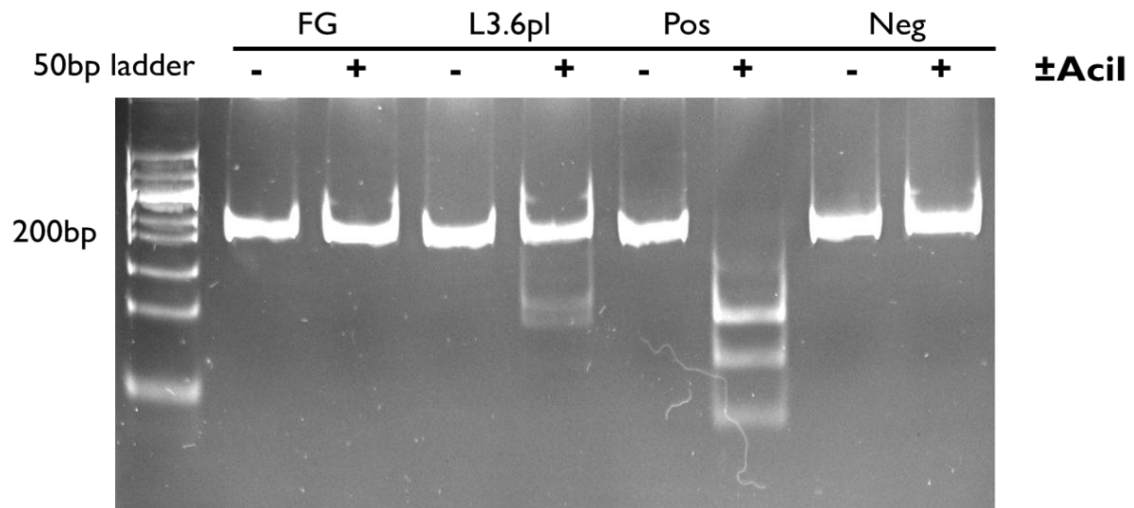


Figure 4.1 DNA methylation within the ZNF300CGI in FG, L3.6pl, as measured by COBRA. Universally methylated (Pos) and non-methylated (Neg) DNA were used as controls. Following bisulfite conversion and amplification, DNA products were subjected to *AciI* digestion and gel electrophoresis. DNA fragmentation is apparent in L3.6pl DNA, as well as the positive control, indicating that *AciI* recognition sites were originally methylated.

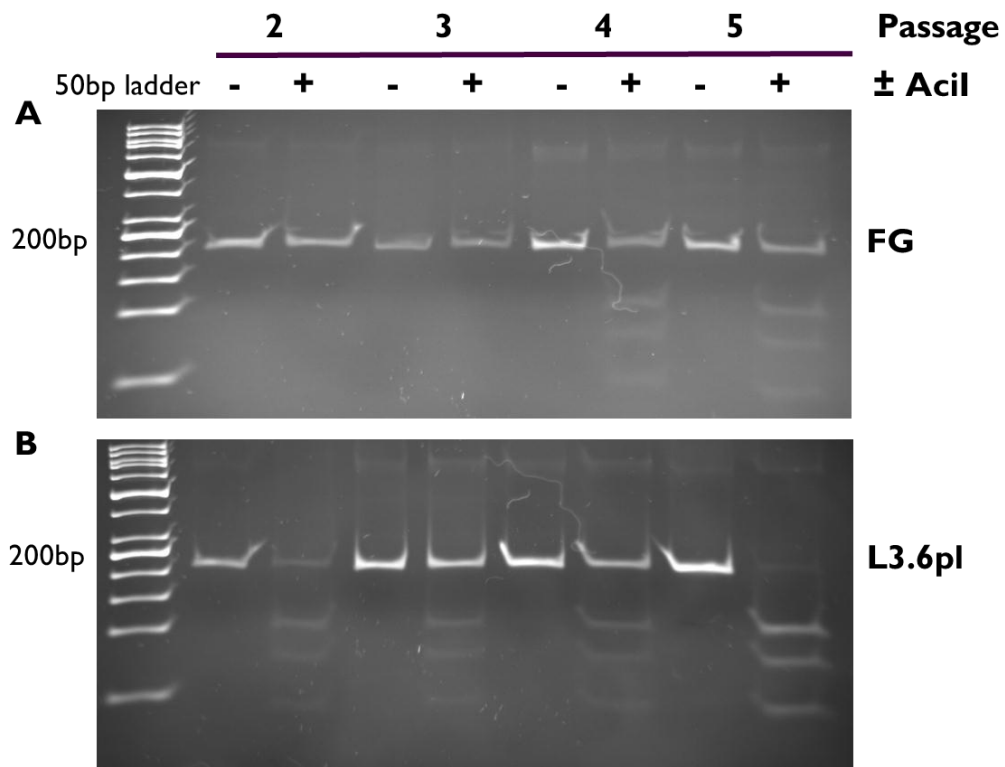


Figure 4.2 Influence of cell passage on DNA methylation within the CGI of ZNF300 using COBRA. Time in culture is represented by increasing passage number. As cell passage increases the degree of fragmentation also increases in FG (A) and L3.6 (B) suggesting that methylation patterns change over time in culture.

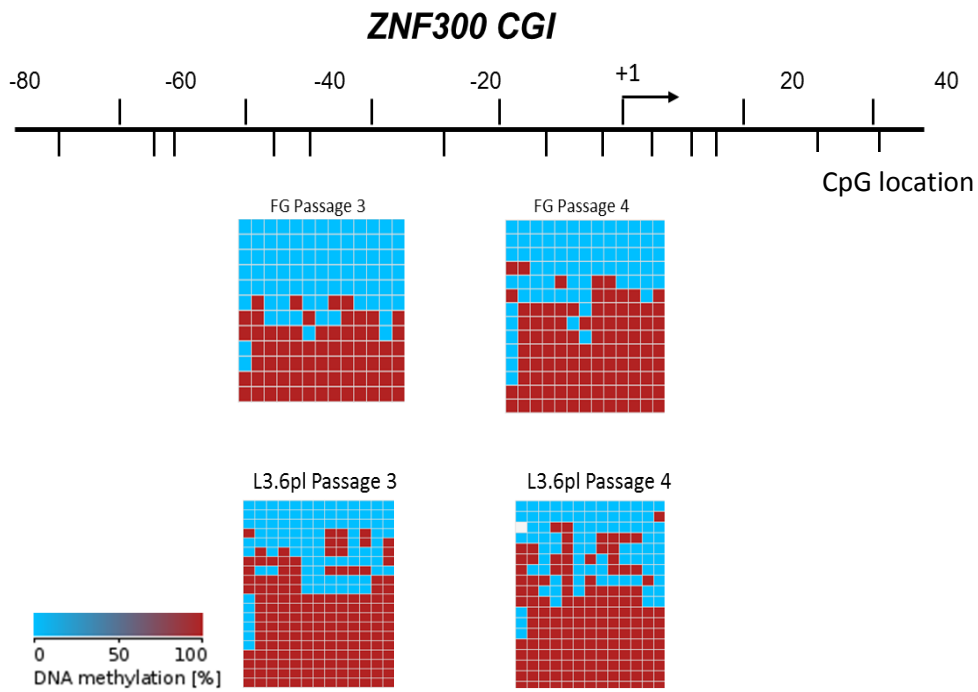


Figure 4.3 Bisulfite sequencing of ZNF300CGI in FG and L3.6pl over cell passage. The relative CpG positions within the ZNF300 CGI are shown above, along with the methylation status at each of the 13CpG. These data reflect DNA methylation changes with increasing cell passage. Each line indicates one sequenced PCR product. Blue squares indicate no observed methylation whereas red squares indicate methylation.

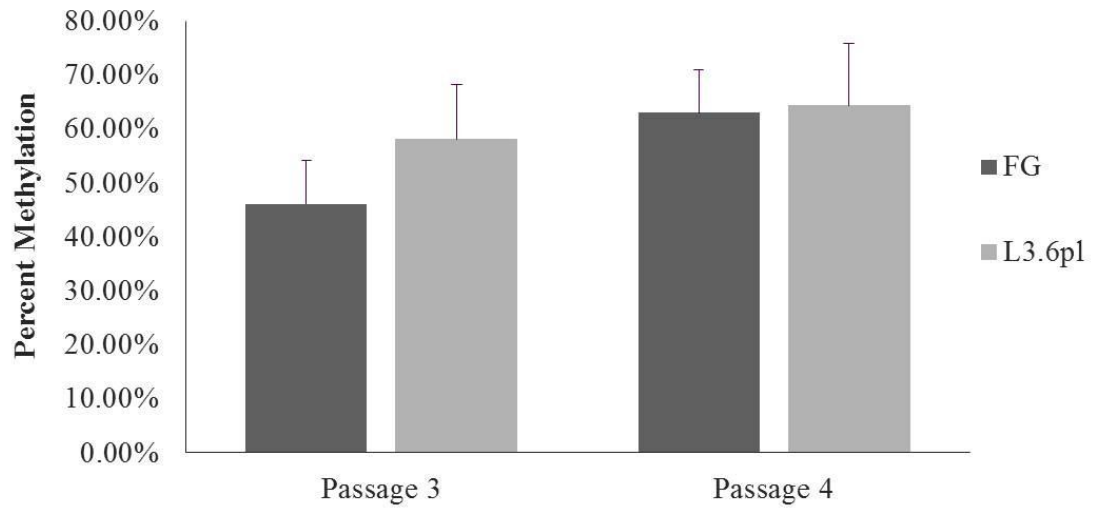


Figure 4.4 Averaged ZNF300 CGI methylation in FG and L3.6pl cells. While the average ZNF300 CGI methylation in both cell lines appeared to change over cell passage, these changes did not reach significance as determined by a Students t-test.

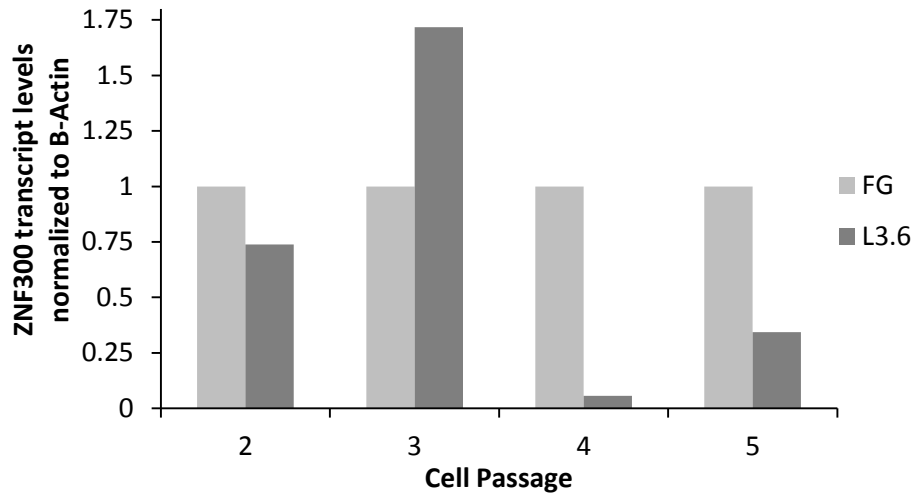


Figure 4.5 ZNF300 transcript levels in FG and L3.6pl quantified via qRT-PCR. In this single experiment, ZNF300 transcripts are normalized to B-Actin. Normalized ZNF300 levels are then shown relative to FG at each passage. There is no conclusive trend in target transcript levels over time; however, these data suggest that ZNF300 transcript levels may be lower in L3.6pl compared to FG at increasing cell passages.

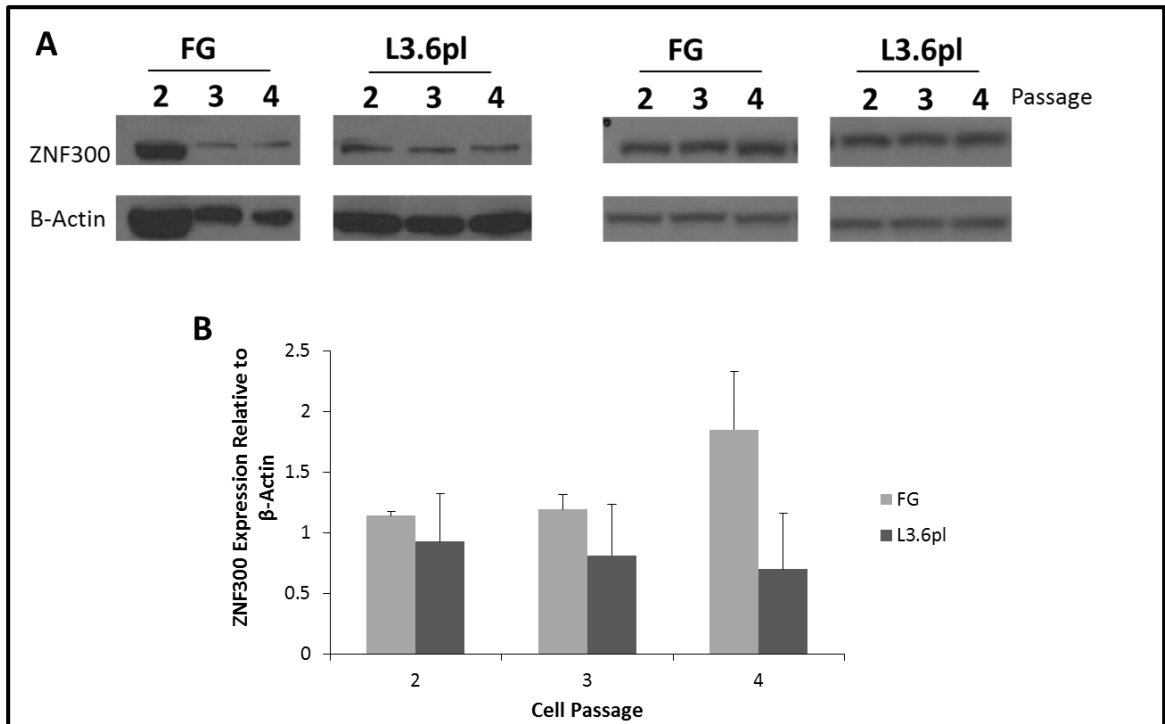


Figure 4.6 ZNF300 expression in FG and L3.6pl cell lines over time in culture. Expression was detected from two independent experiments at passage 2-4 (A). The relative ZNF300 expression normalized to β -Actin was then averaged (B). There was no significant difference in ZNF300 expression with increasing passage in either FG or L3.6pl.

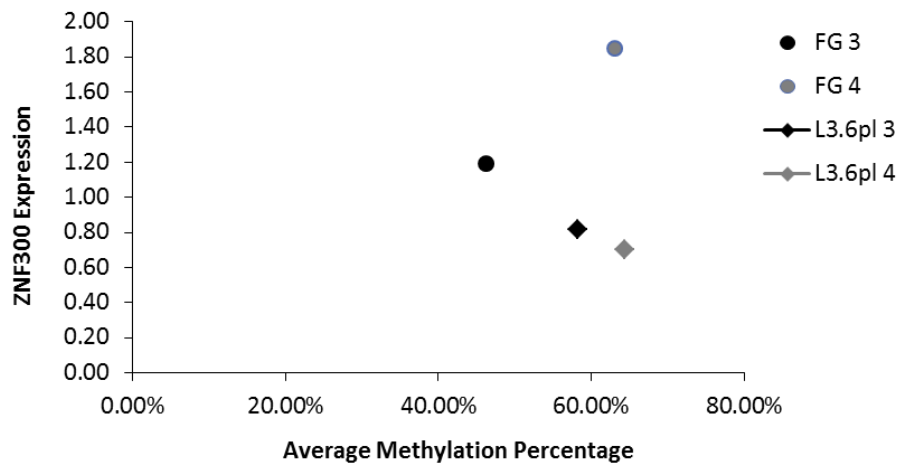


Figure 4.7 Methylation versus ZNF300 expression correlation plot. There was no association found between ZNF300 expression and ZNF300 CGI methylation over time. $p < 0.987$, two-tailed Pearson's correlation analysis.

4.3 Role of ZNF300 in PDAC Metastasis

In aim two I explored the role of ZNF300 in the metastasis of PDAC. To do this, the migratory ability of each cell line was determined by transwell migration assays, an assay that uses chemoattractants to drive the movement of cells across a microporous membrane. Results from migration assays, shown in Figure 4.8, validated expected differences in cell mobility. Specifically L3.6pl cells exhibited an eight-fold increase in the number of migratory cells per view compared to FG cells. It should also be stated that the number of L3.6pl was approximately ten-fold lower than FG in order to accurately quantify the number of migratory cells per view, and thus upon correction for the difference in the number of cells seeded, L3.6pl would exhibit a 80-fold increase in migratory ability.

To determine if ZNF300 contributes the enhanced mobility of L3.6pl cells compared to FG, ZNF300 under was overexpressed via the pRetro-Tet-ON retroviral inducible expression system through the addition of doxycycline. Using L3.6pl cells stably expressing the pRetro-Tet-ON vector (L3.6pl-Tet), exogenous ZNF300 driven under a Tre3G promoter (Tre3G-ZNF300) was transiently infected. These cells are here after referred to as +ZNF300. Both the empty vector Tre3G (EV) and the Tre3G containing Luciferase (+LUC) were independently transfected in L3.6pl-Tet cells as the negative and positive controls, respectively. The experimental approach is illustrated in Figure 4.9 but briefly, following the delivery of Tre3G-ZNF300 or control vectors to L3.6pl-Tet cells, the system was induced by addition of doxycycline

(DOX), a molecule that enabled the Tet-effector protein to effectively bind the Tre3G promoter and induce expression of ZNF300. Both mRNA and protein levels of ZNF300 were measured in all experimental groups over the course of 3, 6, 12, and 24 hours post DOX induction. To test the expression system, L3.6pl cells were transiently infected with +LUC, and luciferase activity was measured via a luciferase assay, as shown in Figure 4.10. While leaky expression was observed, as indicated by the detection of luciferase activity in un-induced conditions, the significantly higher levels of luciferase activity following DOX induction indicate the system is effective. To detect ZNF300 expression following DOX induction, ZNF300 transcript levels were measured by qRT-PCR for +ZNF300 and EV conditions and normalized to L3.6pl-Tet cells that were untreated (UT), and is summarized in Figure 4.11. In DOX-induced-+ZNF300 cells, there was an initial increase in ZNF300 transcripts at hour 3; however this transient induction was followed by a decrease in ZNF300 levels that persisted over 24 hours compared to the UT control. Similar trends were found in the DOX-induced EV cells; specifically, ZNF300 mRNA levels transiently increased at hour 3, then decreased over time. As expected, there were no observed differences in ZNF300 levels among EV cells in the absence of DOX; however, in the absence of DOX, +ZNF300 cells exhibited a gradual increase in ZNF300 transcript levels over time. These data support the previously observed, leaky expression of the p-Retro-Tre3G vector in L3.6pl-Tet cells.

In addition to mRNA levels, changes in ZNF300 protein expression were also examined at the same time points, in two separate experiments. In contrast to ZNF300

transcripts, there was no change in ZNF300 proteins levels under any condition.

Figure 4.12 illustrates the lack of ZNF300 expression changes via western blotting for UT, EV, and +ZNF300 samples at each condition.

To assess potential changes in the migratory ability of L3.6pl-Tet cells under each experimental condition, migration assays were performed at 3, 6, 12, and 24 hours, the results are shown in Figure 4.12. The use of DOX in UT cells seemed to enhance L3.6pl migration; however, there were no effects found in other experimental conditions. Because we failed to induce overexpression of ZNF300, we did not expect to observe changes in the migratory ability of L3.6pl cells. For these reasons, we were unable to determine the functional role that ZNF300 may have in the migratory ability of L3.6pl cells.

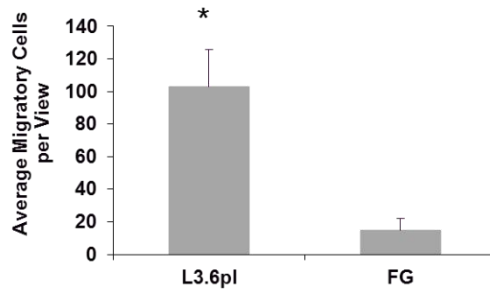
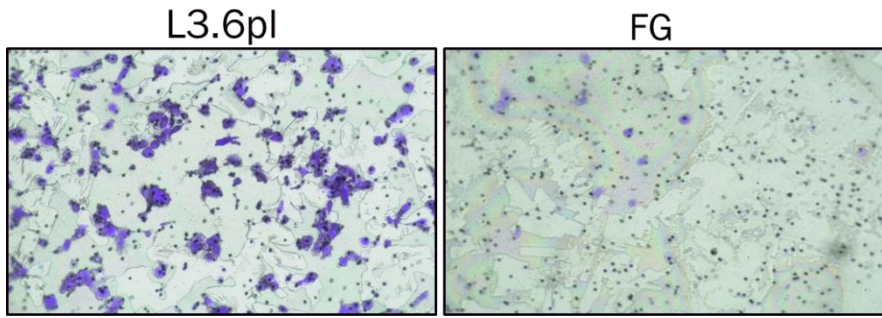


Figure 4.8 Cell migratory abilities of FG and L3.6pl cells via transwell migration assays. Migration assay results reflect the significant increased ability of L3.6pl to migrate across a microporous membrane towards chemoattractants compared to FG. Cells were allowed to migrate for 24 hours whereby they were stained, imaged at 10x (A), and ten images were used to calculate an average number of migrated cells per field (B). $p < 0.001$, Student's t-test.

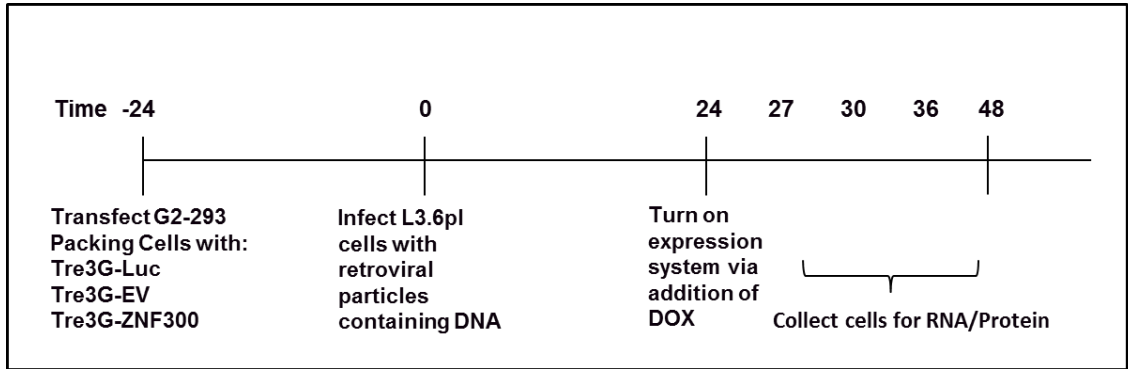


Figure 4.9 Schematic of ZNF300 overexpression in L3.6pl-Tet cells via the Tet-On retroviral expression system. First, G2-293 Packing Cells were transfected with either Tre3G-Luc, EV, or ZNF300. 24hrs later, the viral particles produced by the packing cells were collected and used to infect L3.6pl-Tet cells. 24 hours post infection, DOX was added to facilitate Tet binding to the Tre3G promoter. 3, 6, 12, and 24 hours after the addition of DOX cells were harvested for RNA and protein analysis.

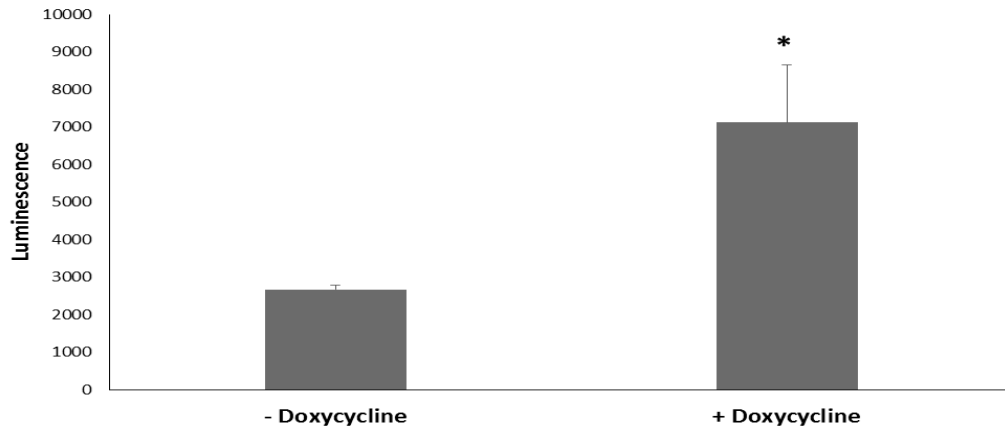


Figure 4.10 Luciferase activity following DOX-induced luciferase expression. Luciferase activity was measured 24hrs post DOX-induction upon the addition of the Luciferase assay reagent to the +LUC-cell lysates. Luciferase activity was present under no-DOX conditions; however, there was a significant increase in activity following the addition of DOX. Each condition was done in triplicate. $p < 0.007$, Student's t-test

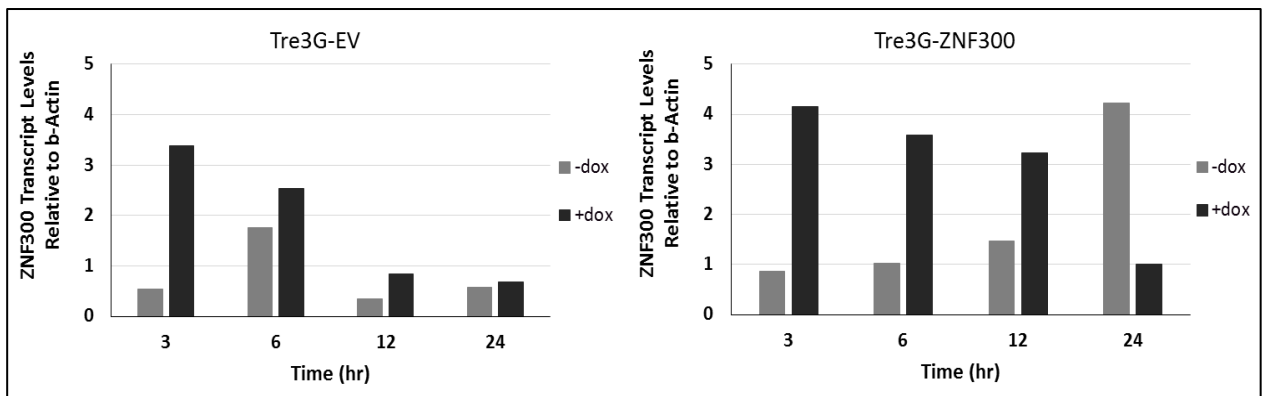


Figure 4.11 ZNF300 transcript levels following DOX induction using the Tet-On retroviral expression system. Both EV and +ZNF300 cells under DOX-induced conditions exhibit a transient increase at 3 hours followed by a steady decline in ZNF300 levels as compared to UT control. Interestingly, in the absence of DOX, there was an increase in ZNF300 levels in +ZNF300 cells over time.

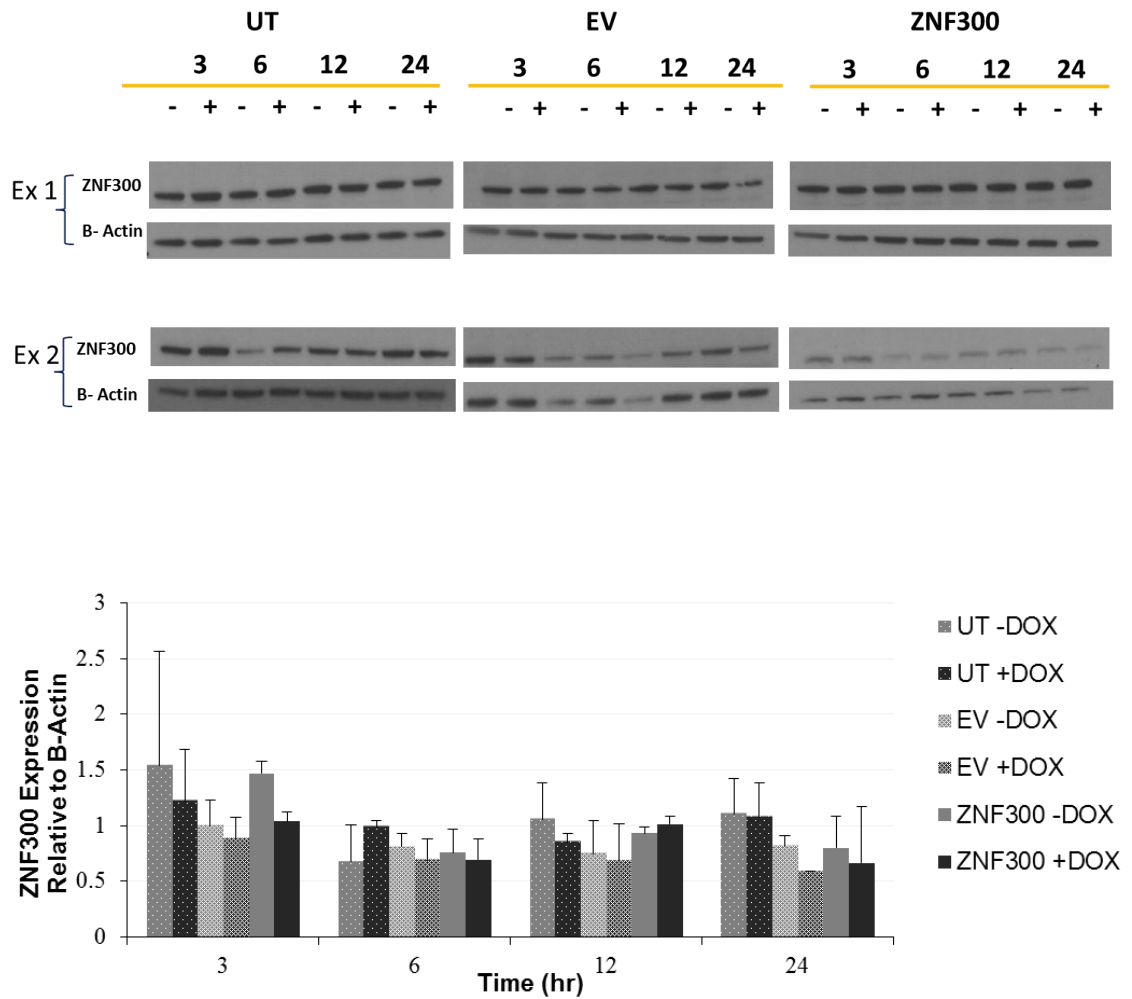


Figure 4.12 ZNF300 expression over time following DOX induction using the Tet-On retroviral expression system. Western blot analysis indicated no change in ZNF300 protein expression in either EV,+ZNF300, or UT cells with or without DOX (A). Averaged quantification of ZNF300 expression normalized to B-Actin from two independent experiments is shown in (B) and illustrates the no change in ZNF300 expression in either EV,+ZNF300, or UT cells with or without DOX.

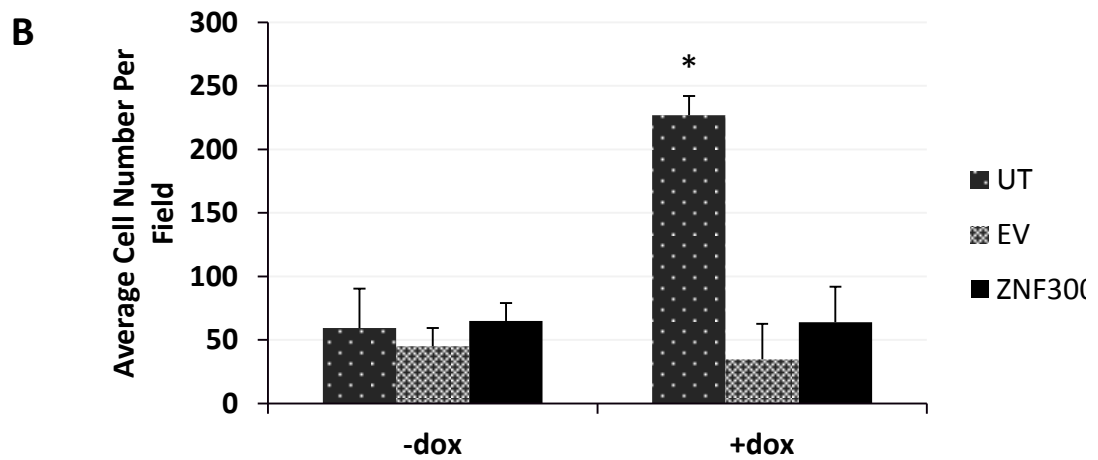
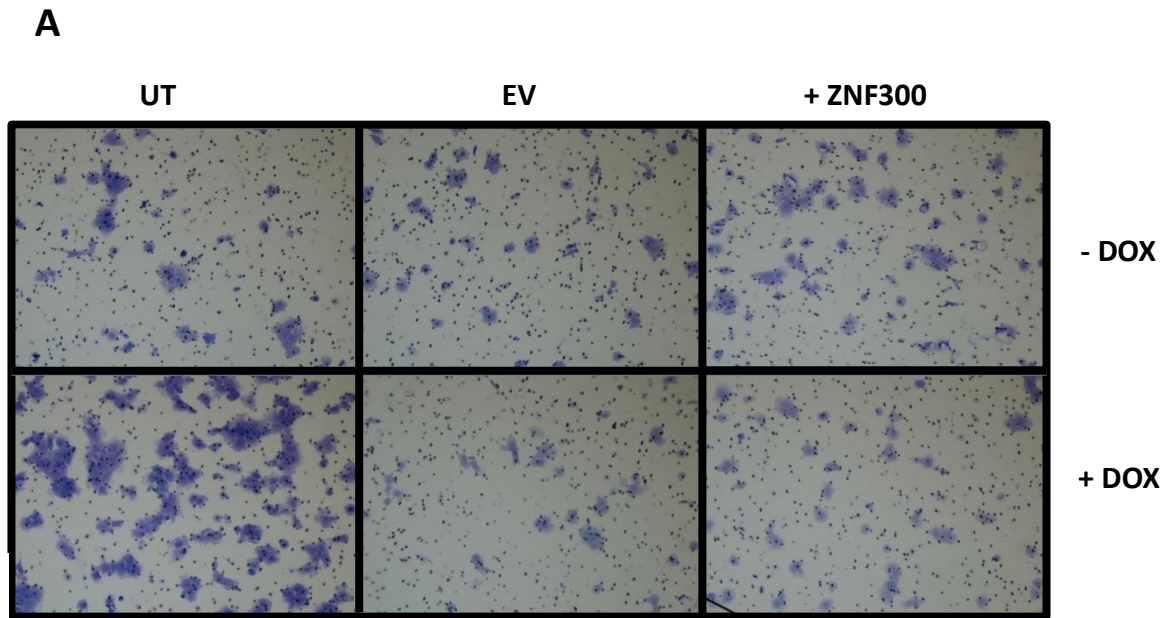


Figure 4.13 Cell migration following DOX-induction of ZNF300 expression using the Tet-On retroviral expression system. There was no change in cell migration in +ZNF300 cells upon addition of DOX; however, there was an increase in cell migration in UT cells under DOX induction (A). Two replicates were performed in this assay. Ten images were taken per condition and averaged migratory cells were counted at 10x (B) $p < 0.01$, Student's t-test.

Chapter 5

DISCUSSION AND FUTURE DIRECTIONS

The first aim of my thesis was to validate the methylation of the ZNF300 CGI. Even though previous lab members had examined methylation within this region, the time cells were cultured, nor the cell passage number, prior to analysis were documented. For these reasons, re-evaluating ZNF300 methylation under our growth conditions, while also tracking the cell passage, was necessary to begin understanding the relationship between ZNF300 promoter methylation and expression. Contrary to the preliminary work, bisulfite sequencing data suggests no difference in methylation among the ZNF300 CGI between the two isogenic cell lines, regardless of cell passage. There are many possible explanations as for why these data are not in agreement. First, both our data and other documented works, demonstrate how culture conditions can affect methylation patterns (Nakamura, Fidler, & Coombes, 2007). For example, our data suggests that FG cells exhibit a fifteen percent increase in ZNF300 methylation at passage four compared to the prior passage. While previous data suggests that ZNF300 is hypermethylated in L3.6pl, the passage of the cells used to generate this data was not recorded. Thus, if the cells used in my studies were expanded from the cells used in the methylation profile, the difference in cultured conditions and increased cell passage number may be an explanation for the conflicting reports of ZNF300 CGI methylation.

Another explanation for contrasting ZNF300 methylation patterns is that two different techniques were used to study DNA methylation. As discussed, the quantification of ZNF300 promoter methylation reported here was measured via sequencing of bisulfite-converted, PCR-amplified DNA. Preliminary methylation data was also collected using PCR-amplification of bisulfite-converted DNA; however, pyrosequencing was employed as the quantification methodology. This technique does not involve cloning the PCR products, but rather sequencing via the synthesis of a complementary strand to single-stranded bisulfite amplified products (Colella, Shen, Baggerly, Issa, & Krahe, 2003) . During synthesis, the release of pyrophosphate results in proportional luminescence measurements and these measurements are used to distinguish between originally methylated, cytosines and non-methylated, thymines (Colella, Shen, Baggerly, Issa, & Krahe, 2003). A study that compared the ability of bisulfite sequencing and pyrosequencing to quantify DNA methylation patterns within a known hypermethylated gene, across multiple cell lines, found that bisulfite sequencing provided a more sensitive quantification of hypermethylated DNA (Reed, Poulin, Yan, & Parissenti, 2010). Despite this finding, it was concluded that pyrosequencing provided a more consistent measurement of numerous methylation patterns across multiple cell lines (Reed, Poulin, Yan, & Parissenti, 2010). A likely factor that contributed to the observed variability of bisulfite sequence data is the use of cloning procedures prior to sequencing. The incidents of cloning bias in sulfite sequencing applications have been reported in many studies (Chhibber & Schroeder, 2008; Reed, Poulin, Yan, & Parissenti, 2010). Both these methods could be skewed by

PCR bias, towards either methylated or non-methylated DNA, which can occur during the amplification process. Incidents of PCR bias can lead to a misrepresentation of methylation patterns within a genomic region (Warnecke et al., 1997). To account for this artifact, the Bisulfite Methylation Analysis (BISMA) software was utilized to identify and discard samples that met clonal criteria. While this step ensured accuracy, it also resulted in a loss of samples that may have been identical due to the hypermethylation of the ZNF300 CGI. In summary, because these methods have reported differences in their ability to quantify DNA methylation, the use of two different analytical methods may explain the contrasting reports of ZNF300 methylation.

As previously mentioned, preliminary work using luciferase promoter assays indicated that the genomic region corresponding to the ZNF300 CGI was important for ZNF300 promoter activity. This data led us to determine if differences in ZNF300 CGI methylation between FG and L3.6pl cells, resulted in differential ZNF300 expression. Because the data indicated no difference in ZNF300 methylation, we expected to find no difference in ZNF300 expression. While mRNA levels did appear to differ in FG and L3.6pl cells, these data were not conclusive due to insufficient experimental replicates. As shown in the previous sections, western blot analysis of ZNF300 expression showed no change in expression between FG and L3.6pl and thus, was consistent with the insignificant differences in ZNF300 CGI methylation between these two lines.

Although the first aim suggested that there may be no difference in the ZNF300 CGI methylation and expression, preliminary immunohistological staining of ZNF300 in PDAC patients suggests that ZNF300 may be silenced upon metastatic advancement of primary pancreatic tumors. For this reason, determining the functional relevance of ZNF300, my objective in aim two, remained biologically relevant. Unfortunately, using Tet-ON pRetroX retroviral expression system to induce ZNF300 expression, lead to no detectable changes in protein expression in L3.6pl-Tet cells. Although doxycycline addition failed to induce ZNF300 expression, one question that was not addressed was if doxycycline led to functional changes of ZNF300. Thus, performing assays to determine if doxycycline induction in cells infected with exogenous ZNF300 led to an increase in ZNF300 function would be another avenue worth exploring.

Little is known about the exact function of ZNF300, however, there is data suggesting that ZNF300 acts as a transcription factor in the immune response gene network (T. Wang et al., 2012). Using q-PCR to detect ZNF300-regulated transcripts would be quick assay that, while the data provided would be indirect, it could serve as an initial screen to determine changes in ZNF300 function. A more direct assay would be to perform DNA binding assays to test for increased binding of ZNF300 to target promoters. Additionally, using ZNF300-regulated genes in reporter assays could also be useful to determine if ZNF300 function increases under the pRetro-X-Tre3G-Tet-ZNF300 expression system. Further characterization of changes in post-translation

modifications of ZNF300 would also be further directions that would contribute towards the understanding of ZNF300 regulation and function.

While the doxycycline-induced ZNF300 expression failed to increase overall ZNF300 protein levels, there were observed changes in ZNF300 transcript levels within ZNF300+ and EV cells. There are many future directions to explore these observations; notably, is to determine the off-target effects of doxycycline to the regulation of ZNF300. The Li laboratory at Wuhan University has provided the only published data projecting the role of ZNF300. Based on their studies, this group hypothesized that ZNF300 aids in the immune response, cell proliferation, and apoptosis (T. Wang et al., 2012). ZNF300 has been proposed to stimulate the genes in the immune response via the NF- κ B pathway (T. Wang et al., 2012). Additionally, doxycycline has been shown to have anti-inflammatory effects, including the downregulation of the cytokines that stimulated the NF- κ B pathway (Bahrami, Morris, & Pourgholami, 2012; L. Han et al., 2014). Taken together, these data reflect the importance of performing additional experiments to elucidate the relationship between doxycycline and ZNF300 as a regulatory protein for the immune response (T. Wang et al., 2012). For example, using this system in another PDAC cell line would allow for validation that the relationship between ZNF300 and doxycycline is gene or cell type specific. If a confounding effect of doxycycline was observed within the ZNF300 gene network, using other expression systems that are not doxycycline dependent may be a more effective expression system to induce ZNF300 overexpression.

While the exact role of ZNF300 is not known, previous studies using HeLa cells have indicated that ZNF300 may act as an oncogene that increases HeLa cell proliferation (T. Wang et al., 2012). More specifically, these studies found that overexpression of ZNF300 led to an increase in NFκB signaling and enhanced ERK phosphorylation (T. Wang et al., 2012). Additionally, xenografts from mice with elevated levels of exogenous ZNF300 exhibited increased tumor formation (T. Wang et al., 2012). These data suggests that, in contrary to what we hypothesized, ZNF300 may act as an oncogene that mediates it's proliferative effects through the MAP kinase and NFκB pathway. Thus, over expressing ZNF300 in multiple PDAC cell lines could be another direction to explore. Additionally, levels of NFκB signaling could be measured in response to ZNF300 stimulation in PDAC cells due to the role of NFκB activation in chronic pancreatitis, an inflammatory disease of the pancreas that is linked to PDAC (H. Huang et al., 2013; N. Li et al., 2013). If NFκB was activated upon ZNF300 overexpression, elucidating the potential role of ZNF300 in chronic pancreatitis would be another direction that could contribute towards the functional role of ZNF300 in PDAC.

REFERENCES

- Aguirre, A. J., Bardeesy, N., Sinha, M., Lopez, L., Tuveson, D. A., Horner, J., . . . DePinho, R. A. (2003). Activated kras and Ink4a/arf deficiency cooperate to produce metastatic pancreatic ductal adenocarcinoma. *Genes & Development*, *17*(24), 3112-3126. doi:10.1101/gad.1158703 [doi]
- Anderson, J. D., Lowary, P. T., & Widom, J. (2001). Effects of histone acetylation on the equilibrium accessibility of nucleosomal DNA target sites. *Journal of Molecular Biology*, *307*(4), 977-985. doi:10.1006/jmbi.2001.4528 [doi]
- Ansari, D., Rosendahl, A., Elebro, J., & Andersson, R. (2011). Systematic review of immunohistochemical biomarkers to identify prognostic subgroups of patients with pancreatic cancer. *The British Journal of Surgery*, *98*(8), 1041-1055. doi:10.1002/bjs.7574 [doi]
- Bahrami, F., Morris, D. L., & Pourgholami, M. H. (2012). Tetracyclines: Drugs with huge therapeutic potential. *Mini Reviews in Medicinal Chemistry*, *12*(1), 44-52. doi:BSP/MRMC/E-Pub/275 [pii]
- Bartholin, L. (2012). Pancreatic cancer and the tumor microenvironment: Mesenchyme's role in pancreatic carcinogenesis. In P. J. Grippo, & H. G. Munshi (Eds.), *Pancreatic cancer and tumor microenvironment* (). Trivandrum (India): Transworld Research Network. doi:NBK98929 [bookaccession]
- Berger, S. L. (2002). Histone modifications in transcriptional regulation. *Current Opinion in Genetics & Development*, *12*(2), 142-148. doi:S0959437X02002794 [pii]
- Bestor, T., Laudano, A., Mattaliano, R., & Ingram, V. (1988). Cloning and sequencing of a cDNA encoding DNA methyltransferase of mouse cells. the carboxyl-terminal domain of the mammalian enzymes is related to bacterial restriction methyltransferases. *Journal of Molecular Biology*, *203*(4), 971-983. doi:0022-2836(88)90122-2 [pii]
- Biankin, A. V., Waddell, N., Kassahn, K. S., Gingras, M. C., Muthuswamy, L. B., Johns, A. L., . . . Grimmond, S. M. (2012). Pancreatic cancer genomes reveal aberrations in axon guidance pathway genes. *Nature*, *491*(7424), 399-405. doi:10.1038/nature11547 [doi]

- Bird, A. (2002). DNA methylation patterns and epigenetic memory. *Genes & Development, 16*(1), 6-21. doi:10.1101/gad.947102 [doi]
- Blackford, A., Serrano, O. K., Wolfgang, C. L., Parmigiani, G., Jones, S., Zhang, X., . . . Hruban, R. H. (2009). SMAD4 gene mutations are associated with poor prognosis in pancreatic cancer. *Clinical Cancer Research : An Official Journal of the American Association for Cancer Research, 15*(14), 4674-4679. doi:10.1158/1078-0432.CCR-09-0227 [doi]
- Bourne, H. R., Sanders, D. A., & McCormick, F. (1990). The GTPase superfamily: A conserved switch for diverse cell functions. *Nature, 348*(6297), 125-132. doi:10.1038/348125a0 [doi]
- Bourne, H. R., Sanders, D. A., & McCormick, F. (1991). The GTPase superfamily: Conserved structure and molecular mechanism. *Nature, 349*(6305), 117-127. doi:10.1038/349117a0 [doi]
- Bronsert, P., Enderle-Ammour, K., Bader, M., Timme, S., Kuehs, M., Csanadi, A., . . . Wellner, U. (2014). Cancer cell invasion and EMT marker expression - a three-dimensional study of the human cancer-host interface -. *The Journal of Pathology*, doi:10.1002/path.4416 [doi]
- Bruns, C. J., Harbison, M. T., Kuniyasu, H., Eue, I., & Fidler, I. J. (1999). In vivo selection and characterization of metastatic variants from human pancreatic adenocarcinoma by using orthotopic implantation in nude mice. *Neoplasia (New York, N.Y.), 1*(1), 50-62.
- Bullock, A. N., Henckel, J., & Fersht, A. R. (2000). Quantitative analysis of residual folding and DNA binding in mutant p53 core domain: Definition of mutant states for rescue in cancer therapy. *Oncogene, 19*(10), 1245-1256. doi:10.1038/sj.onc.1203434 [doi]
- Caldas, C., Hahn, S. A., da Costa, L. T., Redston, M. S., Schutte, M., Seymour, A. B., . . . Kern, S. E. (1994). Frequent somatic mutations and homozygous deletions of the p16 (MTS1) gene in pancreatic adenocarcinoma. *Nature Genetics, 8*(1), 27-32. doi:10.1038/ng0994-27 [doi]
- Caldas, C., & Kern, S. E. (1995). K-ras mutation and pancreatic adenocarcinoma. *International Journal of Pancreatology : Official Journal of the International Association of Pancreatology, 18*(1), 1-6.
- Campbell, S. L., Khosravi-Far, R., Rossman, K. L., Clark, G. J., & Der, C. J. (1998). Increasing complexity of ras signaling. *Oncogene, 17*(11 Reviews), 1395-1413. doi:10.1038/sj.onc.1202174 [doi]

- Carter, H., Samayoa, J., Hruban, R. H., & Karchin, R. (2010). Prioritization of driver mutations in pancreatic cancer using cancer-specific high-throughput annotation of somatic mutations (CHASM). *Cancer Biology & Therapy*, *10*(6), 582-587. doi:12537 [pii]
- Chhibber, A., & Schroeder, B. G. (2008). Single-molecule polymerase chain reaction reduces bias: Application to DNA methylation analysis by bisulfite sequencing. *Analytical Biochemistry*, *377*(1), 46-54. doi:10.1016/j.ab.2008.02.026 [doi]
- Christofori, G. (2006). New signals from the invasive front. *Nature*, *441*(7092), 444-450. doi:nature04872 [pii]
- Colella, S., Shen, L., Baggerly, K. A., Issa, J. P., & Krahe, R. (2003). Sensitive and quantitative universal pyrosequencing methylation analysis of CpG sites. *BioTechniques*, *35*(1), 146-150.
- Collins, M. A., Bednar, F., Zhang, Y., Brisset, J. C., Galban, S., Galban, C. J., . . . Pasca di Magliano, M. (2012). Oncogenic kras is required for both the initiation and maintenance of pancreatic cancer in mice. *The Journal of Clinical Investigation*, *122*(2), 639-653. doi:10.1172/JCI59227 [doi]
- Collins, M. A., Brisset, J. C., Zhang, Y., Bednar, F., Pierre, J., Heist, K. A., . . . di Magliano, M. P. (2012). Metastatic pancreatic cancer is dependent on oncogenic kras in mice. *PloS One*, *7*(12), e49707. doi:10.1371/journal.pone.0049707 [doi]
- Edling, C. E., Selvaggi, F., Buus, R., Maffucci, T., Di Sebastiano, P., Friess, H., . . . Falasca, M. (2010). Key role of phosphoinositide 3-kinase class IB in pancreatic cancer. *Clinical Cancer Research : An Official Journal of the American Association for Cancer Research*, *16*(20), 4928-4937. doi:10.1158/1078-0432.CCR-10-1210 [doi]
- Edwards, Y. H. (1990). CpG islands in genes showing tissue-specific expression. *Philosophical Transactions of the Royal Society of London. Series B, Biological Sciences*, *326*(1235), 207-215.
- Erkan, M., Reiser-Erkan, C., Michalski, C. W., Deucker, S., Sauliunaite, D., Streit, S., . . . Kleeff, J. (2009). Cancer-stellate cell interactions perpetuate the hypoxia-fibrosis cycle in pancreatic ductal adenocarcinoma. *Neoplasia (New York, N.Y.)*, *11*(5), 497-508.
- Eser, S., Schnieke, A., Schneider, G., & Saur, D. (2014). Oncogenic KRAS signalling in pancreatic cancer. *British Journal of Cancer*, doi:10.1038/bjc.2014.215 [doi]
- Esteller, M. (2008). Epigenetics in cancer. *The New England Journal of Medicine*, *358*(11), 1148-1159. doi:10.1056/NEJMra072067 [doi]

- Faltas, B. (2012). Cornering metastases: Therapeutic targeting of circulating tumor cells and stem cells. *Frontiers in Oncology*, 2, 68. doi:10.3389/fonc.2012.00068 [doi]
- Fearon, E. R., & Vogelstein, B. (1990). A genetic model for colorectal tumorigenesis. *Cell*, 61(5), 759-767. doi:0092-8674(90)90186-I [pii]
- Feig, C., Gopinathan, A., Neesse, A., Chan, D. S., Cook, N., & Tuveson, D. A. (2012). The pancreas cancer microenvironment. *Clinical Cancer Research : An Official Journal of the American Association for Cancer Research*, 18(16), 4266-4276. doi:10.1158/1078-0432.CCR-11-3114 [doi]
- Feinberg, A. P., & Tycko, B. (2004). The history of cancer epigenetics. *Nature Reviews.Cancer*, 4(2), 143-153. doi:10.1038/nrc1279 [doi]
- Feinberg, A. P., & Vogelstein, B. (1983). Hypomethylation distinguishes genes of some human cancers from their normal counterparts. *Nature*, 301(5895), 89-92.
- FOULDS, L. (1954). The experimental study of tumor progression: A review. *Cancer Research*, 14(5), 327-339.
- Friess, H., Yamanaka, Y., Buchler, M., Ebert, M., Beger, H. G., Gold, L. I., & Korc, M. (1993). Enhanced expression of transforming growth factor beta isoforms in pancreatic cancer correlates with decreased survival. *Gastroenterology*, 105(6), 1846-1856. doi:S0016508593004093 [pii]
- Gardiner-Garden, M., & Frommer, M. (1987). CpG islands in vertebrate genomes. *Journal of Molecular Biology*, 196(2), 261-282. doi:0022-2836(87)90689-9 [pii]
- Greenman, C., Stephens, P., Smith, R., Dalgliesh, G. L., Hunter, C., Bignell, G., . . . Stratton, M. R. (2007). Patterns of somatic mutation in human cancer genomes. *Nature*, 446(7132), 153-158. doi:nature05610 [pii]
- Hackett, J. A., & Surani, M. A. (2013). DNA methylation dynamics during the mammalian life cycle. *Philosophical Transactions of the Royal Society of London.Series B, Biological Sciences*, 368(1609), 20110328. doi:10.1098/rstb.2011.0328 [doi]
- Han, L., Su, W., Huang, J., Zhou, J., Qiu, S., & Liang, D. (2014). Doxycycline inhibits inflammation-induced lymphangiogenesis in mouse cornea by multiple mechanisms. *PloS One*, 9(9), e108931. doi:10.1371/journal.pone.0108931 [doi]
- Hanahan, D., & Weinberg, R. A. (2000). The hallmarks of cancer. *Cell*, 100(1), 57-70. doi:S0092-8674(00)81683-9 [pii]

- Herreros-Villanueva, M., Hijona, E., Cosme, A., & Bujanda, L. (2012). Mouse models of pancreatic cancer. *World Journal of Gastroenterology : WJG*, *18*(12), 1286-1294. doi:10.3748/wjg.v18.i12.1286 [doi]
- Hezel, A. F., Kimmelman, A. C., Stanger, B. Z., Bardeesy, N., & Depinho, R. A. (2006). Genetics and biology of pancreatic ductal adenocarcinoma. *Genes & Development*, *20*(10), 1218-1249. doi:20/10/1218 [pii]
- Hingorani, S. R., Petricoin, E. F., Maitra, A., Rajapakse, V., King, C., Jacobetz, M. A., . . . Tuveson, D. A. (2003). Preinvasive and invasive ductal pancreatic cancer and its early detection in the mouse. *Cancer Cell*, *4*(6), 437-450. doi:S153561080300309X [pii]
- HOTCHKISS, R. D. (1948). The quantitative separation of purines, pyrimidines, and nucleosides by paper chromatography. *The Journal of Biological Chemistry*, *175*(1), 315-332.
- Hotz, B., Arndt, M., Dullat, S., Bhargava, S., Buhr, H. J., & Hotz, H. G. (2007). Epithelial to mesenchymal transition: Expression of the regulators snail, slug, and twist in pancreatic cancer. *Clinical Cancer Research : An Official Journal of the American Association for Cancer Research*, *13*(16), 4769-4776. doi:13/16/4769 [pii]
- Hruban, R. H., Adsay, N. V., Albores-Saavedra, J., Compton, C., Garrett, E. S., Goodman, S. N., . . . Offerhaus, G. J. (2001). Pancreatic intraepithelial neoplasia: A new nomenclature and classification system for pancreatic duct lesions. *The American Journal of Surgical Pathology*, *25*(5), 579-586.
- Hruban, R. H., Iacobuzio-Donahue, C., Wilentz, R. E., Goggins, M., & Kern, S. E. (2001). Molecular pathology of pancreatic cancer. *Cancer Journal (Sudbury, Mass.)*, *7*(4), 251-258.
- Hruban, R. H., Maitra, A., & Goggins, M. (2008). Update on pancreatic intraepithelial neoplasia. *International Journal of Clinical and Experimental Pathology*, *1*(4), 306-316.
- Hruban, R. H., Takaori, K., Klimstra, D. S., Adsay, N. V., Albores-Saavedra, J., Biankin, A. V., . . . Yonezawa, S. (2004). An illustrated consensus on the classification of pancreatic intraepithelial neoplasia and intraductal papillary mucinous neoplasms. *The American Journal of Surgical Pathology*, *28*(8), 977-987. doi:00000478-200408000-00001 [pii]
- Huang, H., Liu, Y., Daniluk, J., Gaiser, S., Chu, J., Wang, H., . . . Ji, B. (2013). Activation of nuclear factor-kappaB in acinar cells increases the severity of pancreatitis in mice. *Gastroenterology*, *144*(1), 202-210. doi:10.1053/j.gastro.2012.09.059 [doi]

- Ingber, D. E., Madri, J. A., & Jamieson, J. D. (1986). Basement membrane as a spatial organizer of polarized epithelia. exogenous basement membrane reorients pancreatic epithelial tumor cells in vitro. *The American Journal of Pathology*, 122(1), 129-139.
- Itakura, J., Ishiwata, T., Friess, H., Fujii, H., Matsumoto, Y., Buchler, M. W., & Korc, M. (1997). Enhanced expression of vascular endothelial growth factor in human pancreatic cancer correlates with local disease progression. *Clinical Cancer Research : An Official Journal of the American Association for Cancer Research*, 3(8), 1309-1316.
- Jones, P. A., & Baylin, S. B. (2002). The fundamental role of epigenetic events in cancer. *Nature Reviews Genetics*, 3(6), 415-428. doi:10.1038/nrg816 [doi]
- Jones, S., Zhang, X., Parsons, D. W., Lin, J. C., Leary, R. J., Angenendt, P., . . . Kinzler, K. W. (2008). Core signaling pathways in human pancreatic cancers revealed by global genomic analyses. *Science (New York, N.Y.)*, 321(5897), 1801-1806. doi:10.1126/science.1164368 [doi]
- Kanda, M., Matthaei, H., Wu, J., Hong, S. M., Yu, J., Borges, M., . . . Goggins, M. (2012). Presence of somatic mutations in most early-stage pancreatic intraepithelial neoplasia. *Gastroenterology*, 142(4), 730-733.e9. doi:10.1053/j.gastro.2011.12.042 [doi]
- Kanda, M., Sadakari, Y., Borges, M., Topazian, M., Farrell, J., Syngal, S., . . . Goggins, M. (2013). Mutant TP53 in duodenal samples of pancreatic juice from patients with pancreatic cancer or high-grade dysplasia. *Clinical Gastroenterology and Hepatology : The Official Clinical Practice Journal of the American Gastroenterological Association*, 11(6), 719-30.e5. doi:10.1016/j.cgh.2012.11.016 [doi]
- Kastan, M. B., & Berkovich, E. (2007). P53: A two-faced cancer gene. *Nature Cell Biology*, 9(5), 489-491. doi:ncb0507-489 [pii]
- Lamouille, S., Xu, J., & Derynck, R. (2014). Molecular mechanisms of epithelial-mesenchymal transition. *Nature Reviews Molecular Cell Biology*, 15(3), 178-196. doi:10.1038/nrm3758 [doi]
- Li, G., Ji, Y., Liu, C., Li, J., & Zhou, Y. (2012). Reduced levels of p15INK4b, p16INK4a, p21cip1 and p27kip1 in pancreatic carcinoma. *Molecular Medicine Reports*, 5(4), 1106-1110. doi:10.3892/mmr.2012.771 [doi]
- Li, N., Wu, X., Holzer, R. G., Lee, J. H., Todoric, J., Park, E. J., . . . Karin, M. (2013). Loss of acinar cell IKKalpha triggers spontaneous pancreatitis in mice. *The Journal of Clinical Investigation*, 123(5), 2231-2243. doi:10.1172/JCI64498 [doi]

- Li, Y., & Prives, C. (2007). Are interactions with p63 and p73 involved in mutant p53 gain of oncogenic function? *Oncogene*, *26*(15), 2220-2225. doi:1210311 [pii]
- Lienhard, M., Grimm, C., Morkel, M., Herwig, R., & Chavez, L. (2014). MEDIPS: Genome-wide differential coverage analysis of sequencing data derived from DNA enrichment experiments. *Bioinformatics (Oxford, England)*, *30*(2), 284-286. doi:10.1093/bioinformatics/btt650 [doi]
- Liggett, W. H., Jr, & Sidransky, D. (1998). Role of the p16 tumor suppressor gene in cancer. *Journal of Clinical Oncology : Official Journal of the American Society of Clinical Oncology*, *16*(3), 1197-1206.
- Longnecker, D. S., Adsay, N. V., Fernandez-del Castillo, C., Hruban, R. H., Kasugai, T., Klimstra, D. S., . . . Zamboni, G. (2005). Histopathological diagnosis of pancreatic intraepithelial neoplasia and intraductal papillary-mucinous neoplasms: Interobserver agreement. *Pancreas*, *31*(4), 344-349. doi:00006676-200511000-00006 [pii]
- Maitra, A., Fukushima, N., Takaori, K., & Hruban, R. H. (2005). Precursors to invasive pancreatic cancer. *Advances in Anatomic Pathology*, *12*(2), 81-91. doi:00125480-200503000-00006 [pii]
- Maitra, A., & Hruban, R. H. (2008). Pancreatic cancer. *Annual Review of Pathology*, *3*, 157-188. doi:10.1146/annurev.pathmechdis.3.121806.154305 [doi]
- Massague, J., Blain, S. W., & Lo, R. S. (2000). TGFbeta signaling in growth control, cancer, and heritable disorders. *Cell*, *103*(2), 295-309. doi:S0092-8674(00)00121-5 [pii]
- McCarroll, J. A., Naim, S., Sharbeen, G., Russia, N., Lee, J., Kavallaris, M., . . . Phillips, P. A. (2014). Role of pancreatic stellate cells in chemoresistance in pancreatic cancer. *Frontiers in Physiology*, *5*, 141. doi:10.3389/fphys.2014.00141 [doi]
- Miglio, U., Oldani, A., Mezzapelle, R., Veggiani, C., Paganotti, A., Garavoglia, M., & Boldorini, R. (2014). KRAS mutational analysis in ductal adenocarcinoma of the pancreas and its clinical significance. *Pathology, Research and Practice*, *210*(5), 307-311. doi:10.1016/j.prp.2014.01.011 [doi]
- Mihaljevic, A. L., Michalski, C. W., Friess, H., & Kleeff, J. (2010). Molecular mechanism of pancreatic cancer--understanding proliferation, invasion, and metastasis. *Langenbeck's Archives of Surgery / Deutsche Gesellschaft Fur Chirurgie*, *395*(4), 295-308. doi:10.1007/s00423-010-0622-5 [doi]

- Miyaki, M., & Kuroki, T. (2003). Role of Smad4 (DPC4) inactivation in human cancer. *Biochemical and Biophysical Research Communications*, 306(4), 799-804. doi:S0006291X03010660 [pii]
- Moore, L. D., Le, T., & Fan, G. (2013). DNA methylation and its basic function. *Neuropsychopharmacology : Official Publication of the American College of Neuropsychopharmacology*, 38(1), 23-38. doi:10.1038/npp.2012.112 [doi]
- Morgan, R. T., Woods, L. K., Moore, G. E., Quinn, L. A., McGavran, L., & Gordon, S. G. (1980). Human cell line (COLO 357) of metastatic pancreatic adenocarcinoma. *International Journal of Cancer. Journal International Du Cancer*, 25(5), 591-598.
- Morton, J. P., Timpson, P., Karim, S. A., Ridgway, R. A., Athineos, D., Doyle, B., . . . Sansom, O. J. (2010). Mutant p53 drives metastasis and overcomes growth arrest/senescence in pancreatic cancer. *Proceedings of the National Academy of Sciences of the United States of America*, 107(1), 246-251. doi:10.1073/pnas.0908428107 [doi]
- Nakajima, S., Doi, R., Toyoda, E., Tsuji, S., Wada, M., Koizumi, M., . . . Imamura, M. (2004). N-cadherin expression and epithelial-mesenchymal transition in pancreatic carcinoma. *Clinical Cancer Research : An Official Journal of the American Association for Cancer Research*, 10(12 Pt 1), 4125-4133. doi:10.1158/1078-0432.CCR-0578-03 [doi]
- Nakamura, T., Fidler, I. J., & Coombes, K. R. (2007). Gene expression profile of metastatic human pancreatic cancer cells depends on the organ microenvironment. *Cancer Research*, 67(1), 139-148. doi:67/1/139 [pii]
- Neesse, A., Michl, P., Frese, K. K., Feig, C., Cook, N., Jacobetz, M. A., . . . Tuveson, D. A. (2011). Stromal biology and therapy in pancreatic cancer. *Gut*, 60(6), 861-868. doi:10.1136/gut.2010.226092 [doi]
- Nones, K., Waddell, N., Song, S., Patch, A. M., Miller, D., Johns, A., . . . Grimmond, S. M. (2014). Genome-wide DNA methylation patterns in pancreatic ductal adenocarcinoma reveal epigenetic deregulation of SLIT-ROBO, ITGA2 and MET signaling. *International Journal of Cancer. Journal International Du Cancer*, 135(5), 1110-1118. doi:10.1002/ijc.28765 [doi]
- Nowell, P. C. (1976). The clonal evolution of tumor cell populations. *Science (New York, N.Y.)*, 194(4260), 23-28.

- Okano, M., Bell, D. W., Haber, D. A., & Li, E. (1999). DNA methyltransferases Dnmt3a and Dnmt3b are essential for de novo methylation and mammalian development. *Cell*, *99*(3), 247-257. doi:S0092-8674(00)81656-6 [pii]
- Olivier, M., Eeles, R., Hollstein, M., Khan, M. A., Harris, C. C., & Hainaut, P. (2002). The IARC TP53 database: New online mutation analysis and recommendations to users. *Human Mutation*, *19*(6), 607-614. doi:10.1002/humu.10081 [doi]
- Omura, N., Li, C. P., Li, A., Hong, S. M., Walter, K., Jimeno, A., . . . Goggins, M. (2008). Genome-wide profiling of methylated promoters in pancreatic adenocarcinoma. *Cancer Biology & Therapy*, *7*(7), 1146-1156. doi:6208 [pii]
- Oshima, M., Okano, K., Muraki, S., Haba, R., Maeba, T., Suzuki, Y., & Yachida, S. (2013). Immunohistochemically detected expression of 3 major genes (CDKN2A/p16, TP53, and SMAD4/DPC4) strongly predicts survival in patients with resectable pancreatic cancer. *Annals of Surgery*, *258*(2), 336-346. doi:10.1097/SLA.0b013e3182827a65 [doi]
- PHILLIPS, D. M. (1963). The presence of acetyl groups of histones. *The Biochemical Journal*, *87*, 258-263.
- Pylayeva-Gupta, Y., Grabocka, E., & Bar-Sagi, D. (2011). RAS oncogenes: Weaving a tumorigenic web. *Nature Reviews.Cancer*, *11*(11), 761-774. doi:10.1038/nrc3106 [doi]
- Razin, A., & Cedar, H. (1991). DNA methylation and gene expression. *Microbiological Reviews*, *55*(3), 451-458.
- Reed, K., Poulin, M. L., Yan, L., & Parissenti, A. M. (2010). Comparison of bisulfite sequencing PCR with pyrosequencing for measuring differences in DNA methylation. *Analytical Biochemistry*, *397*(1), 96-106. doi:10.1016/j.ab.2009.10.021 [doi]
- Rocco, J. W., & Sidransky, D. (2001). p16(MTS-1/CDKN2/INK4a) in cancer progression. *Experimental Cell Research*, *264*(1), 42-55. doi:10.1006/excr.2000.5149 [doi]
- Rozenblum, E., Schutte, M., Goggins, M., Hahn, S. A., Panzer, S., Zahurak, M., . . . Kern, S. E. (1997). Tumor-suppressive pathways in pancreatic carcinoma. *Cancer Research*, *57*(9), 1731-1734.
- Schutte, M., Hruban, R. H., Geradts, J., Maynard, R., Hilgers, W., Rabindran, S. K., . . . Herman, J. G. (1997a). Abrogation of the rb/p16 tumor-suppressive pathway in virtually all pancreatic carcinomas. *Cancer Research*, *57*(15), 3126-3130.

- Schutte, M., Hruban, R. H., Geradts, J., Maynard, R., Hilgers, W., Rabindran, S. K., . . . Herman, J. G. (1997b). Abrogation of the rb/p16 tumor-suppressive pathway in virtually all pancreatic carcinomas. *Cancer Research*, *57*(15), 3126-3130.
- Schutte, M., Hruban, R. H., Hedrick, L., Cho, K. R., Nadasdy, G. M., Weinstein, C. L., . . . Kern, S. E. (1996). DPC4 gene in various tumor types. *Cancer Research*, *56*(11), 2527-2530.
- Serrano, M., Hannon, G. J., & Beach, D. (1993). A new regulatory motif in cell-cycle control causing specific inhibition of cyclin D/CDK4. *Nature*, *366*(6456), 704-707. doi:10.1038/366704a0 [doi]
- Serre, D., Lee, B. H., & Ting, A. H. (2010). MBD-isolated genome sequencing provides a high-throughput and comprehensive survey of DNA methylation in the human genome. *Nucleic Acids Research*, *38*(2), 391-399. doi:10.1093/nar/gkp992 [doi]
- Shapiro, L., & Weis, W. I. (2009). Structure and biochemistry of cadherins and catenins. *Cold Spring Harbor Perspectives in Biology*, *1*(3), a003053. doi:10.1101/cshperspect.a003053 [doi]
- Shi, C., Fukushima, N., Abe, T., Bian, Y., Hua, L., Wendelburg, B. J., . . . Eshleman, J. R. (2008). Sensitive and quantitative detection of KRAS2 gene mutations in pancreatic duct juice differentiates patients with pancreatic cancer from chronic pancreatitis, potential for early detection. *Cancer Biology & Therapy*, *7*(3), 353-360. doi:5362 [pii]
- Shi, Y., & Massagué, J. (2003). Mechanisms of TGF- β^2 signaling from cell membrane to the nucleus. *Cell*, *113*(6), 685-700.
- Siegel, R., Ma, J., Zou, Z., & Jemal, A. (2014). Cancer statistics, 2014. *CA: A Cancer Journal for Clinicians*, *64*(1), 9-29. doi:10.3322/caac.21208 [doi]
- Son, H., & Moon, A. (2010). Epithelial-mesenchymal transition and cell invasion. *Toxicological Research*, *26*(4), 245-252. doi:10.5487/TR.2010.26.4.245 [doi]
- Takai, D., & Jones, P. A. (2002). Comprehensive analysis of CpG islands in human chromosomes 21 and 22. *Proceedings of the National Academy of Sciences of the United States of America*, *99*(6), 3740-3745. doi:10.1073/pnas.052410099 [doi]
- Tan, A. C., Jimeno, A., Lin, S. H., Wheelhouse, J., Chan, F., Solomon, A., . . . Hidalgo, M. (2009). Characterizing DNA methylation patterns in pancreatic cancer genome. *Molecular Oncology*, *3*(5-6), 425-438. doi:10.1016/j.molonc.2009.03.004 [doi]

- Tian, X., Liu, Z., Niu, B., Zhang, J., Tan, T. K., Lee, S. R., . . . Zheng, G. (2011). E-cadherin/beta-catenin complex and the epithelial barrier. *Journal of Biomedicine & Biotechnology*, 2011, 567305. doi:10.1155/2011/567305 [doi]
- Valastyan, S., & Weinberg, R. A. (2011). Tumor metastasis: Molecular insights and evolving paradigms. *Cell*, 147(2), 275-292. doi:10.1016/j.cell.2011.09.024 [doi]
- Vezeridis, M. P., Meitner, P. A., Tibbetts, L. M., Doremus, C. M., Tzanakakis, G., & Calabresi, P. (1990). Heterogeneity of potential for hematogenous metastasis in a human pancreatic carcinoma. *The Journal of Surgical Research*, 48(1), 51-55.
- Vincent, A., Omura, N., Hong, S. M., Jaffe, A., Eshleman, J., & Goggins, M. (2011). Genome-wide analysis of promoter methylation associated with gene expression profile in pancreatic adenocarcinoma. *Clinical Cancer Research : An Official Journal of the American Association for Cancer Research*, 17(13), 4341-4354. doi:10.1158/1078-0432.CCR-10-3431 [doi]
- Voorneveld, P. W., Stache, V., Jacobs, R. J., Smolders, E., Sitters, A. I., Liesker, A., . . . Hardwick, J. C. (2013). Reduced expression of bone morphogenetic protein receptor IA in pancreatic cancer is associated with a poor prognosis. *British Journal of Cancer*, 109(7), 1805-1812. doi:10.1038/bjc.2013.486 [doi]
- Wang, T., Wang, X. G., Xu, J. H., Wu, X. P., Qiu, H. L., Yi, H., & Li, W. X. (2012). Overexpression of the human ZNF300 gene enhances growth and metastasis of cancer cells through activating NF-kB pathway. *Journal of Cellular and Molecular Medicine*, 16(5), 1134-1145. doi:10.1111/j.1582-4934.2011.01388.x [doi]
- Warnecke, P. M., Stirzaker, C., Melki, J. R., Millar, D. S., Paul, C. L., & Clark, S. J. (1997). Detection and measurement of PCR bias in quantitative methylation analysis of bisulphite-treated DNA. *Nucleic Acids Research*, 25(21), 4422-4426. doi:gka682 [pii]
- Weber, M., Hellmann, I., Stadler, M. B., Ramos, L., Paabo, S., Rebhan, M., & Schubeler, D. (2007). Distribution, silencing potential and evolutionary impact of promoter DNA methylation in the human genome. *Nature Genetics*, 39(4), 457-466. doi:ng1990 [pii]
- Weissmueller, S., Manchado, E., Saborowski, M., Morris, J. P., 4th, Wagenblast, E., Davis, C. A., . . . Lowe, S. W. (2014). Mutant p53 drives pancreatic cancer metastasis through cell-autonomous PDGF receptor beta signaling. *Cell*, 157(2), 382-394. doi:10.1016/j.cell.2014.01.066 [doi]
- Wilentz, R. E., Iacobuzio-Donahue, C. A., Argani, P., McCarthy, D. M., Parsons, J. L., Yeo, C. J., . . . Hruban, R. H. (2000). Loss of expression of Dpc4 in pancreatic

intraepithelial neoplasia: Evidence that DPC4 inactivation occurs late in neoplastic progression. *Cancer Research*, 60(7), 2002-2006.

Xiong, Z., & Laird, P. W. (1997). COBRA: A sensitive and quantitative DNA methylation assay. *Nucleic Acids Research*, 25(12), 2532-2534.

Yamamoto, S., Tomita, Y., Hoshida, Y., Morooka, T., Nagano, H., Dono, K., . . . Aozasa, K. (2004). Prognostic significance of activated akt expression in pancreatic ductal adenocarcinoma. *Clinical Cancer Research : An Official Journal of the American Association for Cancer Research*, 10(8), 2846-2850.

Yin, T., Wang, C., Liu, T., Zhao, G., Zha, Y., & Yang, M. (2007). Expression of snail in pancreatic cancer promotes metastasis and chemoresistance. *The Journal of Surgical Research*, 141(2), 196-203. doi:S0022-4804(06)00501-4 [pii]

Zhang, H. S., Postigo, A. A., & Dean, D. C. (1999). Active transcriptional repression by the rb-E2F complex mediates G1 arrest triggered by p16INK4a, TGFbeta, and contact inhibition. *Cell*, 97(1), 53-61. doi:S0092-8674(00)80714-X [pii]

Zilfou, J. T., & Lowe, S. W. (2009). Tumor suppressive functions of p53. *Cold Spring Harbor Perspectives in Biology*, 1(5), a001883. doi:10.1101/cshperspect.a001883 [doi]

Appendix

A. LETTERS OF PERMISSION

Dear Dr. Phillips,

I am currently finishing my Master's of Science in the Biological Sciences Department at the University of Delaware, and I was wondering if you would give me **permission** to use one of your figures in my **thesis**?

Specifically, my project focused on pancreatic cancer and I was hoping to use your tumor microenvironment figure in my introduction. I copied the figure and article citation below. Please let me know if this would be acceptable.

Thank you so much for your work and for taking the time to consider my request.

[10.3389/fphys.2014.00141](https://doi.org/10.3389/fphys.2014.00141)

Dear Amanda,

You are welcome to use my figure in your **thesis**. Please reference correctly.

Best of luck with your **thesis**..

Kind Regards

Phoebe

Phoebe Phillips, PhD
Senior Lecturer and Group Leader,
Pancreatic Cancer Translational Research Group and
NHMRC CDF Research Fellow,
Room 212, Level 2,
Lowy Cancer Research Centre,
University of New South Wales,
Sydney, NSW, Australia, 2052

Dear Dr. Horii,

I am currently finishing my Master's of Science in the Biological Sciences Department at the University of Delaware, and I was wondering if you would give me **permission** to use one of your figures in my **thesis**? Specifically, my project focused on pancreatic cancer and I was hoping to use your pathology figure in my introduction to show each PanIN stage. I can copied the figure and article citation below. Please let me know if this would be acceptable?

Saiki, Y. and Horii, A. (2014), Molecular pathology of pancreatic cancer. *Pathology International*, 64: 10–19. doi: 10.1111/pin.12114

Dear Amanda Fisher,

I will allow you to use this figure only in the introduction section of your **thesis** with citation information, but copyright belongs to publisher.
You need to ask publisher for **permission**.

Sincerely,

Akira Horii

B. COPYRIGHTED WORKS

JOHN WILEY AND SONS LICENSE TERMS AND CONDITIONS

Nov 10, 2014

This is a License Agreement between Amanda R Fisher ("You") and John Wiley and Sons ("John Wiley and Sons") provided by Copyright Clearance Center ("CCC"). The license consists of your order details, the terms and conditions provided by John Wiley and Sons, and the payment terms and conditions.

All payments must be made in full to CCC. For payment instructions, please see information listed at the bottom of this form.

License Number	3484860925028
License date	Oct 09, 2014
Licensed content publisher	John Wiley and Sons
Licensed content publication	Pathology International
Licensed content title	Molecular pathology of pancreatic cancer
Licensed copyright line	© 2014 The Authors. Pathology International © 2014 Japanese Society of Pathology and Wiley Publishing Asia Pty Ltd
Licensed content author	Yuriko Saiki,Akira Horii
Licensed content date	Jan 29, 2014
Start page	10
End page	19
Type of use	Dissertation/Thesis
Requestor type	University/Academic
Format	Print and electronic

Portion	Figure/table
Number of figures/tables	1
Original Wiley figure/table number(s)	Figure 3
Will you be translating?	No
Title of your thesis / dissertation	ZNF300 may influence the metastatic properties of pancreatic ductal adenocarcinoma
Expected completion date	Jan 2015
Expected size (number of pages)	100
Total	0.00 USD

**NATURE PUBLISHING GROUP LICENSE
TERMS AND CONDITIONS**

Nov 10, 2014

This is a License Agreement between Amanda R Fisher ("You") and Nature Publishing Group ("Nature Publishing Group") provided by Copyright Clearance Center ("CCC"). The license consists of your order details, the terms and conditions provided by Nature Publishing Group, and the payment terms and conditions.

All payments must be made in full to CCC. For payment instructions, please see information listed at the bottom of this form.

License Number	3484851265401
License date	Oct 09, 2014
Licensed content publisher	Nature Publishing Group

Licensed content publication	Nature
Licensed content title	Pancreatic cancer genomes reveal aberrations in axon guidance pathway genes
Licensed content author	Andrew V. Biankin, Nicola Waddell, Karin S. Kassahn, Marie-Claude Gingras, Lakshmi B. Muthuswamy, Amber L. Johns
Licensed content date	Oct 24, 2012
Volume number	491
Issue number	7424
Type of Use	reuse in a dissertation / thesis
Requestor type	academic/educational
Format	print and electronic
Portion	figures/tables/illustrations
Number of figures/tables/illustrations	1
High-res required	no
Figures	Table 2
Author of this NPG article	no
Your reference number	None
Title of your thesis / dissertation	ZNF300 may influence the metastatic properties of pancreatic ductal adenocarcinoma
Expected completion date	Jan 2015
Estimated size (number of pages)	100
Total	0.00 USD